

بسم الله الرحمن الرحيم

Sudan University of Sciences & Technology

College of Graduated Studies

**Measurement of Brain Ventricular Dimensions using
Magnetic Resonance Imaging**

قياس أبعاد التجاويف الدماغية باستخدام التصوير بالرنين المغناطيسي

*A Thesis Submitted for Partial Fulfillment of M.Sc. Degree in
Diagnostic Radiology Technology*

By:

Badawi Mustafa Badawi Suliman

Supervisor:

Dr. Asma Ibrahim Ahmed

Assistant professor

2016

الآية

قال تعالى : (يَا أَيُّهَا الَّذِينَ آمَنُوا إِذَا قِيلَ لَكُمْ تَفَسَّحُوا فِي الْمَجَالِسِ فَافْسَحُوا
يَفْسَحَ اللَّهُ لَكُمْ وَإِذَا قِيلَ انشُرُوا فَانشُرُوا يَرْفَعِ اللَّهُ الَّذِينَ آمَنُوا مِنْكُمْ وَالَّذِينَ
أُوتُوا الْعِلْمَ دَرَجَاتٍ وَاللَّهُ بِمَا تَعْمَلُونَ خَبِيرٌ^{١٦})

(سورة المجادلة 11)

Dedication

To; my mother, the star that lightened my life.

*To the great teacher who sacrifice all for me and my brothers to help and support, my **father.***

Acknowledgment

First of all, I thank Allah the Almighty for helping me complete this project. I thank Dr. Asma Ibrahim Ahmed, my supervisor, for her help and guidance.

I would like to express my gratitude to Dr. Mohamed Ahmed Alfaki, Dr. Kmal Alraih Sanhori and the whole staff of Nelien

medical diagnostic center and Antalya center for their great help and support.

Finally, I would like to thank everybody who helped me to prepare and finish this study.

Table of Content

Topic	Page number
Dedication	I
Acknowledgement	II
Table of contents	III
English Abstract	V
Arabic Abstract	VI
List of abbreviation	VII
List of figures	VIII
List of tables	X
Chapter One: Introduction	
1-1 Introduction	1
1-2 Problem of the study	3
1-3 Objectives	
1-4 Importance of the study	3
1-5 Overview of the study	4
Chapter Two: Literature Review	
2-1 Anatomy of the ventricular system	5

2-2 Histology	19
2-3 Embryology	21
2-4 pathophysiologic variants	23
2-5 Radiological changes in the brain with normal aging	29
2-6 Previous study	35
Chapter Three: Material & Methodology	
3-1 Material	40
3-2 Methodology	41
Chapter Four: Results	
Results and Analysis	46
Chapter Five: Discussion, Conclusions and Recommendations	
5-1 Discussion	57
5-2 Conclusion	62
5-3 Recommendations	63
References	64
Appendices	69

Lest of Figure

Fig.2.1. Lateral view of the ventricular system relative to brain tissue (FitzGelard and Folan 2002)..... 16

Fig.2.2. Cadaveric dissection of the brain at the level of the basal ganglia and thalamus (axial section) [Standring (2008)]..... 16

2.4. Pathophysiologic Variants:..... 18

2.4.1. Hydrocephalus:..... 18

The old classification divides hydrocephalus into 2 types: noncommunicating and communicating. In noncommunicating or obstructive hydrocephalus, the CSF accumulates within the ventricles as a result of an obstruction within the ventricular system (most commonly at the level of cerebral aqueduct). In communicating hydrocephalus, the CSF flows freely through the outflow foramens of the fourth ventricles into the arachnoid space. Current imaging techniques, including computed tomography (CT) scanning and magnetic resonance imaging (MRI) (see the image below), make inferences about the level of obstruction, depending on the presence or absence of ventriculomegaly, especially fourth ventricle dilatation. Fourth ventricle dilatation implies

obstruction distally, usually at the level of the subarachnoid space. A small fourth ventricle suggests obstruction proximal to the fourth ventricle.....	18
.....	18
Fig. 2.4.1. Coronal magnetic resonance image shows a colloid cyst (arrow) in the roof of the third ventricle. The patient has mild hydrocephalus.....	18
Management: Treatment of hydrocephalus is very diverse, including conservative and surgical approaches, depending upon the underlying abnormality and the site of obstruction. In patients with normal pressure hydrocephalus, large-volume lumbar puncture with removal of 40-50 mL of CSF is followed by clinical improvement and high convexity tightness, as seen on CT scan or MRI, indicate a potential benefit with shunting procedures. Isotope cisternography and perfusion tests are additional tests used in selecting surgical candidates. For idiopathic intracranial hypertension, the treatment is directed at lowering CSF pressure and volume. The mainstays of medical treatment include weight reduction, low sodium diet, and diuretics (acetazolamide). A surgical approach is recommended in the setting of failure of standard medical treatment, including shunting, optic nerve fenestration, and, more recently, venous sinus stenting. In obese patients with idiopathic intracranial hypertension, there have been reports that suggest a potential benefit in resolution of symptoms after bariatric surgery. CSF leak and low pressure may occur after lumbar puncture, dural surgical procedures, or as a spontaneous thecal tear. A headache that worsens in the upright position is the clinical hallmark of CSF leaks. Treatment depends on the etiology and includes bedrest, hydration, and an autologous blood patch.....	18
2.5. Radiologic Changes in the Brain with Normal Aging:.....	19
Fig. 1.-Linear ratios used in ventricular measurements.	19
Fig. (3.1) GE Signa HDx 1.5T	20
Fig. (3.2) Axial IR T1-weighted image using a TI of 700ms with the level of the cuts demonstrated in sagittal T1 weighted images (left).....	20
Fig.3.3. Level of fourth ventricles measured at coronal section (right) in our study left image as standard where the measurement is based.....	21
Fig.3.5. Level above the interventricular foramen showed our length of lateral ventricular measures in Right image (axial MRI).....	21
3.2.2. Study Design:.....	21
Figure (4.1) showed the age difference between the three classes of study including gender and age of the child.....	24
Figure (4.2) correlation between the Left lateral ventricular widths with Aqua duct widths in children.....	24
Figure (4.3) correlation between the RT lateral ventricular widths with AD widths in children.....	24
Figure (4.4) correlation between third ventricle widths with AD widths in children. .	24

Figure (4.5) correlation between the Left lateral ventricular widths with AD widths in male population..... 25

Figure (4.6) correlation between the RT lateral ventricular widths with AD widths in male..... 25

Figure (4.7) correlation between the third ventricle widths with AD widths in male. 25

Figure (4.8) Correlation between the lateral ventricular width and length.....25

Figure (4.9) correlation between the right ventricular width and lateral ventricular width..... 26

Figure (4.10) correlation between the right lateral ventricular length and patient age 26

Figure (4.11) simple error bar showed the difference in lateral ventricular length between the male female, and children..... 26

Figure (4.12) simple error bar showed the difference in lateral ventricular width between the male female, and children..... 26

Figure (4.13) simple error bar showed the difference in AD width between the male, female, and children..... 26

Figure (4.14) simple error bar showed the difference in fourth ventricle width between the male female, and children..... 26

Figure (4.15) simple error bar showed the difference in fourth ventricular length between the male female, and children..... 26

Figure (4.16) simple error bar showed the difference in RT ANT horn of lateral ventricle between the male female, and children..... 26

..... 27

Figure (4.17) simple error bar showed the difference in LT ANT horn of lateral ventricle between the male female, and children..... 27

Figure (4.18) simple error bar showed the difference in interventricular canal between the male female, and children..... 27

List of tables

Table 4.1 showed mean STD for the ventricular measurement 46
according to the gender including age and patient weight

List of abbreviations

CSF	Cerebrospinal fluid
MRI	Magnetic resonance imaging
CT	Computed Tomography
Bi	Bilateral
3D	Three dimensional
AP	Anterior to Posterior
RF	Radio frequency
T	Tesla
GE	General electric
ECG	Electrocardiography
IR	Inversion recovery
GRE	Gradient echo sequences
SPGR	Spoiled gradient
TOF	Time of Flight
FSE	Fast spin echo
SSFP	Steady state free precession
FLAIR	Fluid attenuation inversion recovery
EPI	Echo planar imaging
FOV	Field of view
MDCT	Multiple detector computed tomography
LVL	Left Lateral Ventricle Length
LWV	Left lateral Ventricular Width
RVW	Right lateral Ventricular Width
RVL	Right lateral Ventricular Length
ADW	Aqua Duct width
FWV	Fourth Ventricular Width

FVL	Fourth Ventricular length
RA-PL	Right Antero-posterior Horn length
LA-PL	Left Antero-posterior horn length
LAL	Left Anterior Horn length
RAL	Right Anterior horn length
TVW	Third ventricle width
BPD	Biparietal diameter

Abstract:

This study aimed to measure the brain ventricular system dimension in magnetic resonance images using normal MRI caliber in order to establish a reference base for brain ventricles in Sudanese populations also to compare between these measurements in three different classes which are male, female and children. 60 patients with normal MRI brain scan (or clinical indication that not affect the ventricular system) with slice thickness range from 3-5 mm was performed in both Antalya diagnostic center and Nelien medical diagnostic center in period from September 2015- until April 2016. The measurement was performed for Age, Wight of the patient, left Lateral Ventricle Length, left lateral Ventricular Width, right Ventricular Width, Right Ventricular Length, Aqua Duct, Fourth Ventricular Width, Fourth Ventricular length, right Antero-posterior Horn length, Left Antero-posterior horn, left Anterior Horn length, right Anterior horn length, third ventricle width and BPD. And the mean values for these measure was (33.48yers, 67.52kg, 5.3, 1.4, 1.3, 5.4, 0.26,

1.392, 1.05, 8.07, 8.16, 2.48, 2.49, 0.29 and 12.19 cm) for female patients, (38.2yrs, 71.3 kg, 6.0, 1.56, 1.5, 5.9, 0.29, 1.59, 0.9, 8.4, 8.6, 2.6, 2.6, 0.3 and 12.9cm) for male patient and 5.1yrs, 19.7kg, 5.49, 1.09, 1.02, 5.3, 0.25, 1.35, 0.8431, 7.4, 7.3238, 2.18, 2.23, 0.2, and 12.02cm) for child under age of 15years respectively. The correlation reveals that direct significant correlation between the Aqua Duct and the ventricular width and third ventricle higher measurement in male than female in which both higher than child patient.

ملخص الدراسة

هدفت الدراسة الى قياس أبعاد تجاويف السائل النخاعي في صور الرنين المغناطيسية باستخدام مقطع سمكه 3 الى 5 مليمترات, ليتم اعتبارها كقياسات مرجعية للمجتمع السوداني بمختلف فئاته من الذكور والاناث والأطفال. استندت الدراسة على ستين شخصا أظهرت نتائج فحوصاتهم على سلامة التجاويف ولم تكن لديهم أي أعراض قد تؤثر عليها. تمت هذه الدراسة في مركز أنطاليا الطبي ومركز النيلين للتشخيص الطبي في الفترة من سبتمبر 2015 الى ابريل 2016. اشتملت المتغيرات في الدراسة على العمر, الوزن والجنس. بينما كانت القياسات لطول التجويف الجانبي الأيسر وعرضه, طول التجويف الجانبي الأيمن وعرضه, عرض القناة الواصلة بين التجويف الثالث والرابع, طول التجويف الرابع وعرضه, طول التجويف الأمامي الأيمن, طول التجويف الأمامي الأيسر, عرض التجويف الثالث و المسافة بيت السطح الداخلي الأيمن والأيسر

للجمجمة. متوسط قياسات فئة الاناث بالتسلسل المذكور كانت (33.48 عاما, 67.52 كيلوجرام, 5.3 , 1.4 , 1.3 , 5.4 , 0.26 , 1.392 , 1.05 , 8.07 , 8.16 , 2.48 , 2.49 , 0.29 و 12.19). بينما كانت قيم متوسط فئة الذكور بالتسلسل المذكور أعلاه (38.2 عاما , 71.3 كيلو جرام , 6.0 , 1.56 , 1.5 , 5.9 , 0.29 , 1.59 , 0.9 , 8.4 , 8.6 , 2.6 , 2.6 , 0.3 و 12.9). قيم متوسط فئة الأطفال تسلسليا هي (5.1 سنة, 19.7 كيلو جرام , 5.49 , 1.09 , 1.02 , 5.3 , 0.25 , 1.35 , 0.8431 , 7.4 , 7.3238 , 2.18 , 2.23 , 0.2 و 12.02).

أثبتت الدراسة أن عرض القناة الواصلة بين التجويف الثالث والرابع يتناسب طرديا مع عرض التجويف الأيمن والأيسر, وأن عرض التجويف الثالث أكبر عند الرجال من النساء.

Chapter One

1.1. Introduction

The presence of a “hollow” inside the head had been known since ancient times. The origin, content, and function of this hollow, however, was ambiguous. In the third century BC, Herophilus and Erasistratus were able to perform human dissections for the first time in history. Their work led to a better understanding of the ventricles and gave full anatomic description of four “small stomachs,” the ventricles, and their communications. However, they believed that the function of these ventricles was to convert the vital spirit (*pneuma zooticon*), which circulates with the blood from the heart, to the animal (from *anima* means soul) spirit (*pneuma psychikon*). This process was believed to produce thoughts, feelings, and emotions. This belief became more established at the time of Galen. Besides that, Nemesius of Emesa attributed the imagination and its connection with the five senses to the ventricle of the frontal lobe (Schiller 1997).

The ventricles, which became known as “cellulae” until the Renaissance, were counted from three to five in number, and many medical illustrations attempted to demonstrate their appearance in the brain. One of these was by Albertus Magnus in 1506, which represented three cavities surrounded by thin brain tissue. He believed that the functions of these cavities were, from anterior to posterior, imagination, reasoning, and memory. Around 1504, Leonardo da Vinci was the first to make an accurate depiction of the ventricles by performing the first known

ventriculography by injecting molten wax into the ventricles of an ox. However, he also followed the same older belief regarding the functions of the ventricles with only slight modifications. Following Da Vinci's illustrations of the ventricles, anatomists of the Renaissance started to give more attention on studying these cavities, but even in Vesalius's *Fabrica*, the ventricles were described as air containing spaces that fill during inspiration, and contain the animal spirit. In the same period of time, some anatomists, including Nicolo Massa in 1569, opposed the widely held belief of the content of the ventricles. It took almost a century until Constanzo Varolio and Francis Glisson described humor content instead of the classical spirit. This did not end the debate, however. In 1764, Domenico Felice Antonio Cotugno was the first to discover cerebrospinal fluid and to describe the continuity between the ventricles and subarachnoid space. His findings were later confirmed by François Jean Magendie, whose contribution to the discovery of the foramen of Magendie will be described below in addition to the history of ventricular communications)Schiller 1997(.

As ageing advances, the brain undergoes many gross and histopathological changes with regression of the brain tissue leading to the enlargement of the ventricles.) Schiller 1997(Both imaging and autopsy studies revealed that there is correlation with increase in cerebrospinal fluid spaces and reduction in cerebral volume accompanying normal human ageing. (Standring 2008), (Rhoton 2002) Due to these changes that occurs normally

with ageing, the diagnosis of diseases in elderly patients is often complicated. So, the two major changes that may occur in elderly individual without neurologic deficits is enlargement of ventricles and cortical atrophy. However surprisingly, there is lack of clinical, radiologic and pathologic information regarding these changes in humans. The normal ventricular size during life was previously unknown (Schiller 1997).

1.2. Problem of the study:

The introduction of ventricular measurement method has been developed by many authors' like), the evaluation of the pathological condition of CSF containing cavities it's totally or partially depend on the volume or the size of the related ventricles, but the brain ventricle size may vary according to the age, or other normal variants. Therefore, this study was provided a reference measurement for Sudanese groups depending on the MRI imaging which can help in diagnosing of related disease.

1.3. Objectives of the study:

1.3.1. General objectives:

The general aims of this study was to measure the dimension of brain ventricular system in MRI images using MRI caliber in order to establish the reference based measurement for Sudanese population.

1.3.2. Specific objective:

- To measure the length and width of both lateral and fourth ventricles.
- To measure the width of third ventricle.
- To calculate the ventricular to brain ratio.
- To correlate between the lateral ventricles dimensions and the fourth and third ventricles measurement.
- To correlate between the ventricular measurement and different age groups.
- To compare between the measurement of both sex and for different age groups.

1.4. Importance of the study:

The major importance of this study was to provide the base standard for the ventricular size related to the age and sex which help in diagnosing of disease related to ventricular enlargement and introduction of new method of the measurement using MRI rather than CT because it has better demonstration of CSF cavities in T2 and other sequences also multi-planner images can give better evaluation of small ventricles situated in base of the brain.

1.5. Overview of the study:

This study was consisting of five chapters, with chapter one is an introduction; introduce briefly this thesis, problem of study also contains general, specific objectives, significant (important of study and the overview of the study). Chapter two was literature review which contained anatomy, histology, embryology, and pathophysiology of brain ventricular system in addition to the previous studies about the morphological measurement of ventricular system. Chapter three was described the methodology (material, method) was used to achieve the thesis result. Chapter four included presentation (result) of final study; chapter five was discussion, conclusion and recommendations for future scope in addition to references and appendices.

Chapter Two

Literature Review

2.1. Anatomy

The ventricular system of the brain consists of four freely communicating, cerebrospinal fluid (CSF) filled cavities: the two lateral ventricles, the third ventricle, and the fourth ventricle (Figs. 1 and 2). The lateral ventricles are C-shaped cavities that lie deep in each cerebral hemisphere. This shape is thought to be a related to the developmental expansion of the frontal, parietal, and occipital lobes that displace the temporal lobe inferiorly and anteriorly [Standring (2008)].

2.1.1. Lateral ventricles: Each lateral ventricle is divided into a body and atrium, as well as anterior (frontal), posterior (occipital), and inferior (temporal) horns. Each of these parts has medial and lateral walls, a roof, a floor, and an anterior wall [Rhoton (2002)]. The body occupies the parietal lobe and extends from the posterior edge of the foramen of Monro to the point where the septum pellucidum disappears and the corpus callosum and fornix meet. The lateral wall is formed by the caudate nucleus superiorly and the thalamus inferiorly, separated by the striothalamic sulcus, the groove in which the stria terminalis, and the thalamostriate vein course. The medial wall is formed by the septum pellucidum superiorly and the body of the fornix inferiorly. The floor is formed by the thalamus and the roof by the body of the corpus callosum [Standring (2008), Rhoton (2002), Snell (2010), Timurkaynak et.al (1986), Le Gars et.al (2009)].

The body widens posteriorly where it becomes continuous with the atrium. The atrium communicates with the body anteriorly and above the thalamus, with the inferior horn anteriorly and below the thalamus and with the posterior horn posteriorly. The atrium and the occipital horn form a triangular cavity, with the apex in the occipital lobe and the base anteriorly on the pulvinar of the thalamus, which constitutes the anterior wall of the atrium. The roof of the atrium is formed by the body, splenium, and tapetum of the corpus callosum. The floor is formed by the collateral trigone, a triangular area overlying the posterior end of the collateral sulcus. The medial wall is formed by superior and inferior prominences named the bulb of the corpus callosum and calcar avis, respectively. The superior prominence (bulb of the corpus) is formed by the large bundle of fibers called the forceps major, and the inferior prominence (calcar avis) overlies the deepest part of the calcarine sulcus. The anterior part of the lateral wall is formed by the caudate nucleus and the posterior part by fibers of the tapetum of the corpus callosum [Standring (2008), Rhoton (2002), Timurkaynak et.al (1986), Le Gars et.al (2009), Kawashima et.al (2006)].

The occipital (posterior) horn curves posteromedially from the atrium towards the occipital lobe to form a triangular or diamond-shaped cavity. It may vary in size from absent to extending far into the lobe and may vary from side to side. The medial wall is formed by the two prominences: the bulb of the corpus callosum superiorly and the calcar avis inferiorly. The roof and lateral wall

are formed by the tapetum of the corpus callosum, overlaid laterally by the optic radiation, and then the inferior longitudinal fasciculus. The floor is formed by the collateral trigone [Rhoton (2002), Timurkaynak et.al (1986), Le Gars et.al (2009)].

The temporal (inferior) horn, the largest part of the lateral ventricles, extends downward and posteromedially around the pulvinar, and then turns anteriorly in the medial part of the temporal lobe to end 2.5 cm of the temporal pole, just behind the amygdaloid nucleus, which constitutes the anterior wall. The floor is formed by the hippocampus or pes hippocampus and laterally by the collateral eminence, the prominence overlying the collateral sulcus. The medial part of the roof is formed by the inferior surface of the thalamus and the tail of the caudate nucleus separated by the striothalamic sulcus. The lateral part is formed by the tapetum of the corpus callosum, which also sweeps inferiorly to form the lateral wall of the temporal horn. The medial wall is formed by the choroidal fissure, a narrow cleft situated between the inferolateral part of the thalamus, and the fimbria of the fornix [Standring (2008), Rhoton (2002), Timurkaynak et.al (1986), Le Gars et.al (2009)].

The frontal (anterior) horn extends anteriorly from the interventricular foramen into the frontal lobe. It has a roughly triangular shape on the coronal section. The medial wall is formed by the septum pellucidum, separating the frontal horns on both sides. The anterior wall and roof are formed by the genu of the corpus callosum. The lateral wall is formed by the head of the

caudate nucleus, and the narrow floor by the rostrum of the corpus callosum [Standring (2008), Rhoton (2002), Timurkaynak et.al (1986), Le Gars et.al (2009)].

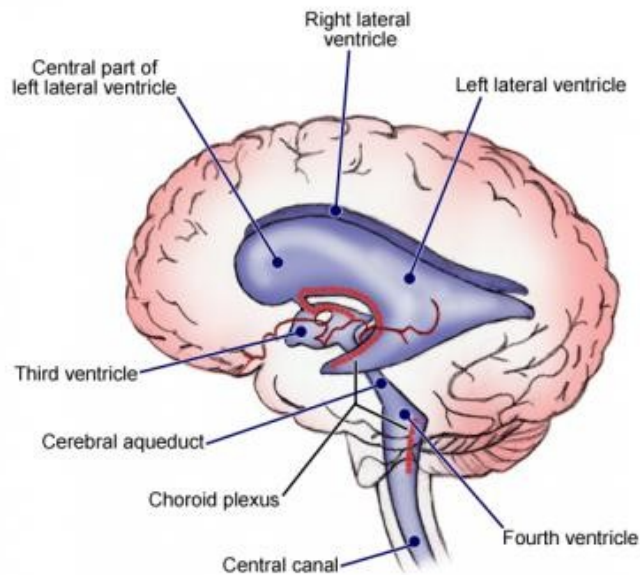


Fig.2.1. Lateral view of the ventricular system relative to brain tissue (FitzGelard and Folan 2002)

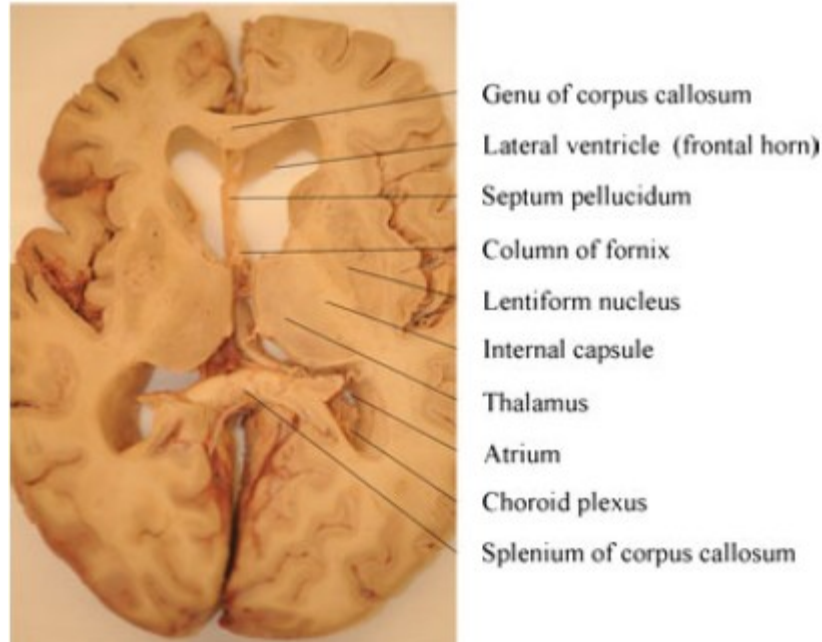


Fig.2.2. Cadaveric dissection of the brain at the level of the basal ganglia and thalamus (axial section) [Standring (2008)].

Kremen et.al (2012), in 2010, revised and reported on previous studies on the heritability of the size of the lateral ventricles in twin cases. They concluded that lateral ventricular volume is heritable, and that its heritability does increase with age from childhood to at least late middle age. As with the case of the cerebral hemispheres themselves, asymmetry of the lateral ventricles exists. The incidence of this asymmetry is 5-12 %, which make it relatively a common entity. Asymmetry of the lateral ventricles can be expected with an underlying pathological condition, but in the absence of underlying pathology, the presence of this asymmetry raises many questions [Kiroglu et.al (2008)]. However, the underlying cause of this asymmetry is still

obscure. In a study by McRae et.al in 1968, they found that the left occipital horn was longer than the right in 57 % of cases, and the right occipital horn was longer in 13 %. According to them, this, in most, is related to brain dominance, as the left occipital horn is longer in right handed adults, and the right is longer in left-handers. Strauss and Fitz (1980), in 1983, studied the occipital horns of 75 subjects, age 5 months to 18 years. They found that in 29(38.7 %) of the cases, the left horn was longer than the right and the right was longer in 13 (17 %) of the cases. Furthermore, they reported an association between early brain lesions in the first year of life and this asymmetry, mainly in the cases of a longer right occipital horn, as 85 % of them reported history of brain injury in early life, compared to 46 % with longer left horns. In 1983, in a sonographic examination of brains of 66 human neonates with gestational ages of 28-44 weeks, Horbar et.al (1983), reported asymmetry in the body of the lateral ventricle. This asymmetry could be found as early as the first postnatal day in infants with a gestational ages low as 28 weeks. The body of the left lateral ventricle was larger in 31.8 % of the neonates, whereas the right body was larger in only 6.1%. According to them, this asymmetry could result from intrauterine or postnatal compression of the skull. Erdogan et al. [Erdogan et.al (2004)] studied the effects of gender and handedness on the size and asymmetry of the lateral, third, and fourth ventricle. They stated that both handedness and underhandedness gender handedness interaction were significant factors influencing the volumes of the

right and left lateral, third, and fourth ventricles, but gender was not significant. The mean volumes of the right lateral and third ventricles were significantly larger in right-handers than in left-handers, but the mean volumes of the left-lateral and fourth ventricles did not exhibit any significant handedness difference. Degree and character of right-to left asymmetry also changes with various kinds of diseases and abnormalities. For instance, in patients with autism, highly localized reductions in volume in the left frontal and occipital horns of the lateral ventricles have been reported [Vidal et.al (2008)]. In addition, the degree of asymmetry may change in patients with schizophrenia in relation to sex [Graham et.al (2006)]. Kiroglu et.al (2008) studied the association of the asymmetry of the lateral ventricle with clinical and structural pathologies, and they concluded that an asymmetric lateral ventricle represents a normal anatomic variation and has a relatively lower risk for accompanying disorders in cases of mild or moderate degree asymmetries without septal deviation or diffuse enlargement. However, with severe degree of asymmetries and the presence of septal deviation or diffuse enlargement, it should not be considered normal.

2.1.2. Foramen of Monro: The interventricular foramen (of Monro) is named, according to most authors, after Alexander Monro Secundus (1733-1817). Some authors [Morton (1954)], however, ascribe it to Alexander Monro Primus (1697-1767). In his earliest work, in 1783, Monro (Secundus) [Monro (1783)] stated that this foramen has been described before, but never

illustrated. However, a thorough investigation by Sharp [Monro (1783)] in 1961 doubts his claim. At the end of his study, Sharp concluded, “The present writer feels strongly that there is no justification for the retention of the eponymous term ‘foramen of Monro’ as a synonym for the interventricular foramen of the modern terminology for two reasons: firstly, because Monro added nothing of value to the pre-existing description of the foramen, and secondly because he actually misinterpreted the nature of the communication between the third and lateral ventricles” [Monro (1783)].

The interventricular foramen forms the communicating canal between the lateral ventricle on either side and the third ventricle at the junction of the roof and the anterior wall. It has a diameter of 3–4 mm, and is bounded anteriorly by the junction of the body and the columns of the fornix and posteriorly by the anterior pole of the thalamus, and has a posterior concavity. The size and shape of the foramina of Monro depend on the size of the ventricles: If the ventricles are small, each foramen is a crescent-shaped opening bounded anteriorly by the concave curve of the fornix and posteriorly by the convex anterior tubercle of the thalamus. As the ventricles enlarge, the foramen on each side becomes rounder. The structures that pass through the foramen are the choroid plexus, the distal branches of the medial posterior choroidal arteries, and the thalamostriate, superior choroidal, and septal veins [Rhoton (2002), Le Gars (2009)]. Congenital atresia of the foramen of Monro is infrequently reported in literature

[Bhagwati (1964), Taboada et.al (1979), Blatt and Berkmen (1969)].

2.1.3. Third ventricle: The third ventricle is a narrow, funnel-shaped, unilocular, midline cavity located at the center of the head. It communicates with the lateral ventricles through the interventricular foramen of Monro on its anterosuperior aspect, and with the cerebral aqueduct of Sylvius on its posteroinferior aspect. The roof of the third ventricle forms a gentle upward arch, extending from the foramen of Monro anteriorly to the suprapineal recess posteriorly. It has four layers: one neural layer, the uppermost layer, formed by the body of the fornix anteriorly and by the crura and the hippocampal commissure posteriorly, the septum pellucidum is attached to the upper surface of the body of the fornix. Below the neural layer, there are two thin membranous layers of tela choroidea and a layer of blood vessels between the sheets of tela choroidea. The anterior wall of the third ventricle is formed, from superior to inferior, by the diverging columns of the fornix, foramina of Monro, the transversely orientated anterior commissure, lamina terminalis, optic recess, and optic chiasm [Rhoton (2002)]. The anterior half of the floor is formed by diencephalic structures, and the posterior half is formed by mesencephalic structures. When viewed from below, the structures forming the floor include, from anterior to posterior, optic chiasm and its recess, the infundibulum of the hypothalamus and its narrow funnel-shaped recess, the tuber cinereum of the hypothalamus, the mamillary bodies, the

posterior perforated substance, and most posteriorly the part of the tegmentum of the midbrain located above the medial aspect of the cerebral peduncles. At the junction of the floor and the anterior wall, a small, angular, optic recess extends into the optic chiasm [Standring (2008), Rhoton (2002)]. In their experimental study on the normal anatomy and some pathological changes of the third ventricle, Corrales et al. [Corrales and Torrealba (1976)] have described three portions in the floor of the third ventricle: The first or premammillary portion is the thinnest and extends from the infundibulum to the premammillary sulcus. The second or interpeduncular portion is slightly thicker and extends from the post mammillary recess to the posterior border of the interpeduncular space. The third or peduncular portion is the thickest segment and corresponds to the portion lying on the cerebral peduncles and it extends to the aqueduct of Sylvius. The optic recess is a small, angular cavity situated between the junction of the anterior wall and the floor of the third ventricle. Its floor or posteroinferior wall is formed by the optic chiasm, which at the same time separates its cavity from the infundibulum. Its anterior or anterosuperior wall is formed by the lamina terminalis, which has a posterior curving insertion in the superior aspect of the optic tract. The insertion of the lamina terminalis may be more anteriorly or posteriorly located in the superior surface of the chiasm. The optic recess extends laterally in both sides following to a small extent the posterior lateral curving insertion of the lamina terminalis in the optic tract. This fact makes the

optic recess broader as compared with the infundibulum. The lateral border of the optic recess is formed by the inferior part of the “area praeoptica” of the hypothalamus. At its superoposterior aspect, the optic recess communicates with the cavity of the third ventricle [Corrales and Torrealba (1976)]. Normal variations in the anatomy of the optic recess and subsequently optic chiasm have been reported [Bull (1956)]. In addition, conditions of persisting embryonic infundibular recess, albeit rare, have been recognized [Steno et.al (2009)].

The posterior wall of the third ventricle is formed, from above to below, by the suprapineal recess, the habenular commissure, the pineal body and its recess, the posterior commissure, and the aqueduct of Sylvius. The suprapineal recess projects posteriorly between the upper surface of the pineal gland and the lower layer of tela choroidea in the roof. The pineal recess projects posteriorly into the pineal body between the two laminae of the pineal gland [Rhotonm(2002)]. Suprapineal recess is usually a small cavity that lies above the habenular commissure. Posteriorly, it extends near the corpus callosum to the vicinity of the quadrigeminal cistern. It is 2-3 mm in height and length. Dilatation of the suprapineal recess is the most common variation in the third ventricle, and according to Krokfors et al., it is present in 4 % of the cases they studied. Occasionally, both the height and the length may exceed 10 mm, and lengths even up to 40 mm have been encountered. A large suprapineal recess has not been considered to have any pathological significance. In the case of hypertensive

hydrocephalus, the suprapineal recess may become greatly distended, and it has indeed been termed the “pressure diverticulum” of the third ventricle [Krokhors et.al (1967)].

The upper part of the lateral wall of the ventricle is formed by the medial surface of the anterior two thirds of the thalamus, and the lower part is formed by the hypothalamus anteriorly and the subthalamus posteriorly. The boundary between the thalamus and hypothalamus is marked by the ill-defined hypothalamic sulcus, which extends horizontally on the ventricular wall between the interventricular foramen of Monro and the cerebral aqueduct [Standring (2008)]. The superior limit of the thalamic surfaces is marked by narrow, raised ridges, known as the striae medullaris thalami. These striae extend forward from the habenulae along the superomedial surface of the thalamus near the attachment of the lower layer of the tela choroidea [Rhoton (2002)]. The upper halves of the lateral walls of the third ventricle are joined by an interthalamic adhesion, or massa intermedia, a band of gray matter, which extends from one thalamus to the other. It is present in approximately 75 % of brains and located 2.5–6.0 mm (average, 3.9 mm) posterior to the foramen of Monro [Standring (2008), Rhoton (2002)].

2.1.4. Aqueduct of Sylvius: As with most of the brain structures, the first introduction of a canal between the third and fourth ventricles was made by Galen. According to some authors [Longatti et.al (2007)], the first recent illustration of the cerebral aqueduct can be traced by to Leonardoda Vinci. However, the first

description of this canal was done by Berengarius Carpensis in 1521. Later on, Vesalius clearly described the aqueduct in his book, *Fabrica*, in 1543. Jacobus Sylvius, a famous French anatomist and a blind follower of Galen, was born in 1478, and he was the teacher of Vesalius. His book *Isagoge* was published in 1555, and in the book, we can find a clear description of the aqueduct. This later publication of his work has obscured the merits of Sylvius, who had probably seen the cerebral aqueduct much earlier than his student Vesalius. In 1663, a Dutch anatomist named François de le Bœe (or Franciscus Sylvius in the Latinized form) also described the same structure in his book *Disputations* and probably the term aqueduct of Sylvius (aka *aqueductus Sylvii*) can be ascribed to him. The term aqueduct, derived from the Latin word *aqueductus*, was first used by Arantius in 1587 [Leite Dos Santos et.al (2004)].

In 1855, and based on his histological studies, von Gerlach [Gerlach (1858)] subdivided the Sylvian aqueduct into three parts and proclaimed that the shape of the aqueduct is different from site to site on cross sections. Turkewitsch [Turkewitsch (1935), Turkewitsch (1936)], on the other hand, recognized five portions, namely, the *aditus aquaeductum* or *aditus aquaeducti*, anterior part, *ampulla*, *genu*, and posterior part. The anterior part and the *genu* form the first and second constrictions surrounding the enlarged *ampulla*, and formed by the superior and inferior *colliculi*, respectively [Longatti et.al (2007), Longatti et.al (2008)]. Woollam and Millen [Woollam and Millen (1953)] considered this

subdivision rather elaborate and suggested a division into three parts: Pars Anterior, Ampulla, and Pars Posterior [Flyger and Hjelmquist (1957)]. The aqueduct is the narrowest part of the ventricular system and the most common site for blockade, and it is approximately 18 mm long [Snell (2010)]. The antrum of the aqueduct is triangular in shape, with the floor located dorsally, and formed by the posterior commissure; the other two limbs are formed by the central gray matter of the midbrain, mainly by the two red nuclei [Rhoton (2002), Woollam and Millen (1953)].

Broman (1927) and Bickers and Adams (1949) stated the size of the lumen of the aqueduct decreases progressively from the second fetal month to birth due to the effect of the surrounding nuclear system and neural fibers development. Spiller (1916) found that the aqueductal lumen continues to decrease in size with age much like the central canal of the spinal cord. Flyger and Hjelmquist (1957), and based on experimental study, concluded that the CSF pressure within the lumen of the aqueduct does not allow any shrinkage and that the size increases with age. They did not mention, however, whether this is due to general old age atrophy or to a reduction in the size of the surrounding nuclear masses and fiber tracts. They also included that the cross-sectional area of the aqueduct differs from site to site and patient to patient and may range from 0.40 to 9.84 mm² [Flyger and Hjelmquist (1957)]

2.1.5. Fourth ventricle: The fourth ventricle is a broad, tent-shaped midline cavity located at the center of the posterior fossa

between the brainstem and the cerebellum. It lies ventral to the cerebellum, dorsal to the pons and upper half of the medulla, and medial to the cerebellar peduncles. It is connected rostrally with the cerebral aqueduct, caudally with the central canal of the spinal cord, inferoposteriorly with the cisterna magna through the foramen of Magendie, and laterally with the cerebellopontine angles through the foramina of Luschka. The fourth ventricle has a roof, a floor, and two lateral recesses. Its widest part is at the pontomedullary junction where a lateral recess on both sides extends to the lateral border of the brain stem [Standring (2008), Matsushima et.al (1982)].

The apex of the tent-shaped cavity extends from its narrow rostral end at the level of the aqueduct to its narrow caudal end at the level of the foramen of Magendie. Between these two ends, the roof expands laterally and posteriorly to reach its peak (fastigium) at the level of the lateral recesses, before it tapers again caudally. The fastigium divides the roof into superior and inferior parts. The superior part is formed by the medial borders of the two superior cerebellar peduncles and a connecting sheet of white matter called the superior medullary velum, which is continuous with the white matter of the cerebellum and is covered dorsally by the lingula of the superior vermis. The inferior part of the roof is formed by the inferior medullary velum, which consists of a thin sheet devoid of nervous tissue and formed by the ventricular ependyma and its posterior covering of the pia mater of the tela choroidea. At the level of the inferior medullary velum, just below

the nodule of the cerebellum, a median aperture known as the foramen of Magendie, connects the ventricle with the cisterna magna [Standring (2008), Snell (2010), Matsushima et.al (1982)]. The floor of the fourth ventricle is diamond, or rhomboid in shape, called the rhomboid fossa. The rostral two third of the floor lies behind the pons, and the caudal third lies behind the superior half of the medulla. The upper tip of this diamond cavity is located at the level of the aqueduct and the inferior end, the obex, at the antrum of the central canal, opposite to the foramen of Magendie. The lateral angles open through the lateral recesses and the foramina of Luschka. The floor is divided into three parts: superior or pontine part, intermediate or junctional part, and inferior or medullary part. The superior part is triangular in shape, its apex is formed by the aqueduct, the base is formed by imaginary line connecting the two cerebellar peduncles, and the two limbs are formed by the medial surface of the two cerebral peduncles. The intermediate part is a strip between the lower margin of the cerebellar peduncles and the site of insertion of the tela choroidea at the taenia of the fourth ventricle just below the lateral recesses. The inferior part is triangular in shape, its apex lies caudally and opposite to the foramen of Magendie, the base of the triangle is at the lower margin of the intermediate part, and the lateral limbs are formed by the taenia of fourth ventricle. The floor is divided longitudinally from the rostral tip to the caudal tip into symmetrical halves by the median sulcus. On each side of this sulcus, there is an elevation, the medial eminence, which is

bounded laterally by another sulcus, the sulcus limitans. Lateral to the sulcus limiting, there is an area known as the vestibular area overlying the vestibular nuclei [Standring (2008), Snell (2010), Matsushima et.al (1982)].

The sulcus limitans is discontinuous, and it is more prominent at two points, or dimples, in the pontine and medullary parts of the floor. The pontine dimple is called the superior fovea, and the medullary dimple is called the inferior fovea. At the level of the superior fovea, each medial eminence is represented by the facial colliculus, a slight swelling produced by the fibers from the motor nucleus of the facial nerve looping over the abducens nucleus. Caudal to the inferior fovea, each medial eminence has three triangular areas: The most medial is the hypoglossal triangle, overlying the hypoglossal nucleus. Lateral to this is the vagal triangle, overlying the dorsal motor nucleus of the vagus. The third is the area postrema, a narrow area between the vagal triangle and the lateral margin of the ventricle, just rostral to the opening into the central canal. The inferior part of the vestibular area also lies lateral to the vagal triangle. Strands of nerve fibers, the stria medullaris, derived from the arcuate nuclei, emerge from the median sulcus and pass laterally over the medial eminence and the vestibular area and enter the inferior cerebellar peduncle to reach the cerebellum. At the rostral tip of the sulcus limitans, at the lateral margin, there is a bluish-gray area, produced by a cluster of nerve cells containing melanin pigment and norepinephrine; the cluster of cells is called the substantia

ferruginea and is more commonly known as locus coeruleus [Standring (2008), Snell (2010), Matsushima et.al (1982)]. The lateral recesses were discovered by Bochdalek in 1849 and mistakenly thought to be blind extensions of the fourth ventricle, but they were later correctly revealed as channels communicating with the subarachnoid space by Luschka in 1855. The lateral recesses are narrow, curved pouches formed by the union of the roof and the floor of the fourth ventricle. They extend laterally below the cerebellar peduncles, which open through the foramina of Luschka into the cerebellopontine angle along the V-shaped cerebellopontine fissure. The ventral wall of each lateral recess is formed by the junctional part of the floor and the rhomboid lip, a sheet like layer of neural tissue that extends laterally from the floor and attach to the tela choroidea to form a pouch at the center extremity of the lateral recess. The dorsal wall is formed by the peduncle of the flocculus interconnecting the inferior medullary velum and the flocculus. As the lateral recess extends towards the cerebellopontine angle, the contribution of the inferior medullary velum and tela choroidea reduces and the rhomboid lip takes its place. The rostral wall is formed by the caudal margin of the cerebellar peduncles, and the caudal wall is formed by the tela choroidea [Matsushima et.al (1982), Sharifi et.al (2009)].

In 1828, François Magendie (1828) presented his findings regarding the cerebrospinal fluid at the Academy of Sciences in Paris, titled *Mémoire Physiologiquesur le Cerveau*. His descriptions

included an opening in the midline of lower part of the roof of the fourth ventricle, later named after him, that is variable in size and wide enough to admit the point of the finger [Rogers (1931), Tubbs et.al (2008)]. The presence of this opening has been confirmed later by Luschka (1855), Key and Retzius (1875), and others. However, it has been also denied by many authors, including Todd in 1847, Virchow in 1854, Reichert in 1861, and many others. In 1931, Rogers documented this controversy and confirmed the presence of this aperture, but stated that it is not a normal foramen, but rather a deformity in the roof of the ventricle. He believes, however, that his finding does not contradict with Magendie's [Rogers (1931)].

Hubert von Luschka, a German anatomist, was the first to describe the foramina of Luschka in 1855. Luschka commented and confirmed the presence of the foramen of Magendie and described an open communication between the fourth ventricle and the subarachnoid space in the cerebello-medullary and cerebellopontine cisterns at the outer margins of the fourth ventricle. His findings, although denied by some authors, were later confirmed by many anatomists including Key and Retzius in 1875 [Sharifi et.al (2009), Tubbs et.al (2011)]. The rhomboid lip, which is initially caudal, becomes the medial lip of the foramen of Luschka. Immediately anterior to the foramen sites the origins of the glossopharyngeal and vagus nerves, whereas the acoustic striae, cochlear nerve, and flocculus are just anterosuperior [Jean et.al (2003)].

2.2. Histology:

The term ependyma, which was first introduced by Virchow more than a hundred years ago, is used to describe the special type of cuboidal to columnar epithelial cells that line the ventricular system of the brain and central canal of the spinal cord [Mestres (1998)]. The ependymal lining of the cerebral ventricles constitutes a layer of heterogeneous cells that are variably modified. In the lateral ventricles, two main types of ependymal cells can be identified: ciliated and non-ciliated cells. These cells lack the characteristic tight junctions presenting in the choroid plexus. In the ventrolateral wall of the third ventricle, a third type of cells can also be identified, the tanocytes, which were first described by Horst Mann in 1954 [Mestres (1998)].

Tanocytes, of which almost four types have been identified, have unique elongated cytoplasmic processes that extend from the ventricular lining toward the surrounding neuropils, where they enwrap blood vessels or terminate on neurons, glia, or the external glial limitans. Their function was of interest to the scientists after their suggested role in neuroendocrine connection between the CSF and the hypophysial-portal vasculature to affect the adenohipophysial function along with the hypothalamus. This function was mainly attributed to the tanocytes located along the floor and lateral walls of the fundibular recess. Some authors suggested that the hypothalamic hormones first go the CSF and then to the portal system by way of the tanocytes. Others suggested a complementary function to the hypothalamus, as the

tanycytes may selectively absorb certain substances from the CSF (e.g., end organ hormones) and transport them to vessels or neurons that affect the function of the adenohypophysis. A counter-transport function may also present, where substances from the neuronal or vascular secretion may be transported to the CSF. However, the definitive evidence and importance of this function are still not clear. Other possible function of the tanycytes in the brain may include modifying the ionic concentrations in the extracellular space of the periventricular zone and, hence, the membrane properties of neuronal processes. Beneath the ependymal layer, the sub ependymal glial cells are found, where the ependymal cells exhibit numerous in folding's that interdigitate with adjacent astrocyte processes and blood vessels and contributes to the formation of the blood-brain barrier [Mestres (1998)].

However, this barrier does not present in ever part of the ventricular system. In certain parts along the third and fourth ventricles, the barrier is ineffective or totally absent, which allows almost free communication between these structures and the blood. These structures, which are collectively known as circumventricular organs, include the pineal gland, median eminence, subfornical organ, area postrema, sub commissural organ, organum vasculosum of the lamina terminalis, and posterior lobe of the pituitary gland [Bruni et.al (1985), Gabrion et.al (1998), Bruni (1998), Ross and Pawlina (2006)].

2.3. Embryology

Following neural tube closure, three dilatations, the primitive brain vesicles, are formed on the cephalic end of the neural tube. These vesicles, from cephalic to caudal, are the prosencephalon (forebrain), mesencephalon (midbrain), and rhombencephalon (hindbrain). At the fifth week of gestation, the prosencephalon gives rise to the telencephalon (cerebral hemispheres) and the diencephalon. The rhombencephalon also gives rise to the metencephalon (cerebellum and pons) and the myelencephalon (medulla oblongata). Cavities remain inside these developing vesicles, communicating with the lumen of the neural tube and represent the future ventricles. The cavity of the rhombencephalon is the fourth ventricle, the cavity of the diencephalon is the third ventricle, and those of the telencephalon are the lateral ventricles. The lumen of the mesencephalon connects the third and fourth ventricles and later becomes narrower and known as the cerebral aqueduct [Sadler (2006)].

During the early phase of their development, the ventricles undergo massive expansion with faster growth compared to the surrounding brain tissue. Upon reaching the maximum ventricle/brain ratio, with the ventricle assuming the adult size, the brain begins to outpace the ventricular growth and leads to a change of the ventricular configuration to the adult form. This process proceeds in a caudal to rostral direction [Lowery (2008)].

The precise position and unique shape of the brain ventricles is proposed to be controlled directly or indirectly by a number of patterning genes and their products. These genes received more

extensive study in animal models, including chick embryos and zebrafish. One of these genes is the ventral neural signaling morphogen Sonic Hodgehog (Shh) that is secreted by the notochord. Early separation of the notochord from the brain may lead to loss of Shh expression and subsequent ventricular collapse. Other examples include h1x1 gene, and zic family of genes. The mechanism by which these genes might affect the ventricular pattern is not well understood [Lowery (2008)].

One theory, introduced by His, proclaimed that the shape of the ventricles is a result of uneven cellular proliferation, migration, and differentiation throughout the neural tube, and controlled by the patterning genes intrinsic to different brain regions. Programmed cell death has also been found to counter the effect of cellular proliferation and control the proper ventricular formation. Beside this spatial morphogenesis of the ventricles, much specific tissue changes are also genetically regulated. This includes cells shape changes and cytoskeleton formation, development of the intercellular adhesion and tissue maintenance, and the epithelial anchoring and support with the extracellular matrix formation. The embryonic CSF, which is suggested to be secreted by neuroepithelial and non-neuroepithelial (vascular) sources, constitutes another important factor in the development of the ventricles. It plays this role mainly by creating a continuous intraluminal pressure that inflates the ventricles. It also contains large number of proteins and

growth factors that affects the surround cells proliferation and differentiation [Lowery (2008)].

2.4. Pathophysiologic Variants:

Intracranial pressure is the pressure within the closed craniospinal compartment, which encompasses 3 main components: brain parenchyma, intracranial cerebrospinal fluid (CSF), and cerebral blood volume. An increase in CSF pressure happens as a result of an increase in the intracranial volume (eg, tumors), blood volume (with hemorrhages), or CSF volume (eg, hydrocephalus). Blocking the circulation of the CSF leads to dilatation of the ventricular system upstream to the level of obstruction, defined as hydrocephalus.

2.4.1. Hydrocephalus:

The old classification divides hydrocephalus into 2 types: noncommunicating and communicating. In noncommunicating or obstructive hydrocephalus, the CSF accumulates within the ventricles as a result of an obstruction within the ventricular system (most commonly at the level of cerebral aqueduct). In communicating hydrocephalus, the CSF flows freely through the outflow

foramens of the fourth ventricles into the arachnoid space. Current imaging techniques, including computed tomography (CT) scanning and magnetic resonance imaging (MRI) (see the image below), make inferences about the level of obstruction, depending on the presence or absence of ventriculomegaly, especially fourth ventricle dilatation. Fourth ventricle dilatation implies obstruction distally, usually at the level of the subarachnoid space. A small fourth ventricle suggests obstruction proximal to the fourth ventricle.



Fig. 2.4.1. Coronal magnetic resonance image shows a colloid cyst (arrow) in the roof of the third ventricle. The patient has mild hydrocephalus.

Current terminology classifies all types of hydrocephalus as obstructive at some level, except for the rare cause of CSF

overproduction associated with choroid plexus papilloma. Intraventricular obstructive hydrocephalus refers to hydrocephalus resulting from an obstruction within the ventricular system (eg, aqueductal stenosis). The continuous production of the CSF leads to dilatation of one or more ventricles, depending on the site of obstruction. In the acute obstruction phase, transependymal flow of CSF may occur. The gyri are flattened against the skull. If the skull sutures are not calcified, such as in children younger than age 2 years, the head may enlarge. Extraventricular obstructive hydrocephalus indicates an obstruction outside the ventricles (eg, at the level of arachnoid villi, as a result of previous bleeding, infection, or inflammation, which results in thickening of the arachnoid and decreased absorption of the CSF).

2.4.1.1. Symptoms/signs: Hydrocephalus causes symptoms mainly due to increased intracranial pressure. The symptoms and findings vary with age. Clinical features of hydrocephalus in infants include irritability, lethargy, poor feeding, vomiting, and failure to thrive. In older children and adults, morning headache associated with vomiting, diplopia, gait dysfunction as a result of stretching of the paracentral corticospinal fibers, coordination problems, and impairment in the higher functions are seen. Macrocephalus, cracked pot sound with percussion, separation of sutures, frontal bossing, or occipital prominence is usually seen in children with hydrocephalus that developed before the closing of the cranial vault. Papilledema, exudates or hemorrhages, and

optic atrophy may be seen upon funduscopic examination in children or adults. Enlargement of the blind spot is also noted. Diplopia is usually caused by bilateral sixth nerve palsy due to increased intracranial pressure. A paralysis of the up gaze or partial Parinaud syndrome (setting sun sign) is seen as a result of pressure on the superior colliculus or tectum. Other findings include hormonal changes as a result of third ventricle dilatation and pressure on the hypothalamic-pituitary structures, cognitive dysfunction, changes in personality may be seen, and, occasionally, seizures. Posterior fossa tumors may cause transforaminal herniation of the cerebellar tonsils with neck stiffness.

2.4.1.2. Etiopathophysiology: The etiologies and pathogenesis of hydrocephalus include overproduction, blockage, or diminished absorption. The only known etiology of excess production is choroid plexus papilloma, which is a rare tumor seen in less than 2% of childhood tumors.

Etiologies of hydrocephalus secondary to blockage or diminished absorption include developmental abnormalities, trauma, tumors, infectious, inflammatory, and idiopathic. Solid tumors produce hydrocephalus by obstruction of the ventricles, whereas nonsolid tumors (e.g., leukemia, carcinomatous infiltration) impair CSF absorption within the subarachnoid space.

The following are some causes of obstruction at specific locations in the ventricular system: Foramen of Monro obstruction may be

caused by a suprasellar mass (e.g., glioma, arachnoid cyst, craniopharyngioma), septum pellucidum tumor, colloid cyst, or tuberous sclerosis, Third ventricle obstruction may result from a colloid cyst, large hypothalamic-optic or thalamic glioma, or suprasellar mass, Cerebral aqueduct obstruction may be the result of aqueductal stenosis, vascular malformations (e.g., arteriovenous malformations or vein of Galen aneurysm), ventriculitis, ependymitis, or tumors (e.g., pineal, brainstem, cerebellar, or mesencephalic), Obstruction at the level of fourth ventricle may be caused by posterior fossa tumors, hemorrhage, or ventriculitis, Obstruction of the fourth ventricle foramina of Luschka and Magendie may be due to a Dandy-Walker malformation, arachnoid cyst, infection (eg, ventriculitis, meningitis), or cerebellar tumors and obstruction at the level of subarachnoid space is usually caused by hemorrhage (subarachnoid or subdural), meningitis, and, rarely, by Chiari malformation

2.4.2. Congenital hydrocephalus:

Congenital hydrocephalus has an incidence of 0.4-0.8 per 1000 live births and stillbirths, with noncommunicating hydrocephalus as the most common form of hydrocephalus in fetuses. Aqueductal stenosis is the most common cause of congenital hydrocephalus, whereas mass lesions are the most common cause of aqueductal obstruction during childhood. Other causes of congenital noncommunicating hydrocephalus include the following: Dandy-Walker malformation, which consists of a

markedly dilated fourth ventricle associated with failure of the foramen of Magendie to open, aplasia of the posterior cerebellar vermis, heterotopias of the inferior olivary nuclei, pachygyria, agenesis of the corpus callosum, and other abnormalities, Klippel-Feil syndrome, defined by obstructive hydrocephalus at the level of fourth ventricle associated with malformation of the craniocervical skeleton (This condition may be associated with Chiari malformation and basilar impression.), Chiari malformation, Congenital brain tumors, most common being astrocytoma, medulloblastoma, teratoma, and choroid plexus papilloma (These tumors are more often supratentorial and midline, usually compressing the cerebral aqueduct.), Vein of Galen malformation, Walker-Warburg syndrome, a congenital syndrome characterized by hydrocephalus, agyria, and retinal dysplasia, with or without encephalocele, associated with congenital muscular dystrophies, *Hydrancephaly, porencephaly, and schizencephaly:* Hydrancephaly results from replacement of the brain parenchyma by the CSF. Causes include a failure in normal brain development, intrauterine disease destroying the normal brain tissue, or untreated progressive obstructive hydrocephalus. Porencephaly refers to hemispheric cysts resulting from the destruction of immature brain parenchyma, which may or may not communicate with the lateral ventricle and subarachnoid space. Schizencephaly is the term used for a cleft in the brain parenchyma that is lined with dysplastic gray matter, extending from the ventricles to the cortex.

Normal pressure and arrested hydrocephalus: The uniformly dilated ventricles with normal CSF pressure are classified as normal pressure hydrocephalus (NPH). Arrested hydrocephalus may represent a form of normal pressure hydrocephalus. Normal pressure hydrocephalus may be accompanied by gait disorder, incontinence, and dementia in elderly patients. The etiology is presumed to be idiopathic, resulting in increased resistance to CSF absorption across the arachnoid villi. A remote history of trauma, infection, or subarachnoid hemorrhage may be elicited occasionally. CT scanning or MRI reveals uniform ventricular dilatation out of proportion to the cortical atrophy, with periventricular lucencies.

Idiopathic intracranial hypertension: (IIH)

(also known as pseudotumor cerebri) is a diagnosis of exclusion. Predominantly seen in young, obese women (age 20-40 y; female-to-male ratio, 3:1), it manifests with headaches and visual disturbances; in the most severe cases, visual loss may result. The eye examination findings are related to increased intracranial pressure and include papilledema, retinal hemorrhages, exudates, enlargement of the blind spot, and sixth cranial nerve palsies. On CT scan or MRI, the ventricular system appears normal. Empty sella may be seen in a small percentile of patients. Lumbar puncture reveals elevated CSF pressure greater than 250 mm H₂O, with normal CSF composition.

Management: Treatment of hydrocephalus is very diverse, including conservative and surgical approaches, depending upon the underlying abnormality and the site of obstruction. In patients with normal pressure hydrocephalus, large-volume lumbar puncture with removal of 40-50 mL of CSF is followed by clinical improvement and high convexity tightness, as seen on CT scan or MRI, indicate a potential benefit with shunting procedures. Isotope cisternography and perfusion tests are additional tests used in selecting surgical candidates. For idiopathic intracranial hypertension, the treatment is directed at lowering CSF pressure and volume. The mainstays of medical treatment include weight reduction, low sodium diet, and diuretics (acetazolamide). A surgical approach is recommended in the setting of failure of standard medical treatment, including shunting, optic nerve fenestration, and, more recently, venous sinus stenting. In obese patients with idiopathic intracranial hypertension, there have been reports that suggest a potential benefit in resolution of symptoms after bariatric surgery. CSF leak and low pressure may occur after lumbar puncture, dural surgical procedures, or as a spontaneous thecal tear. A headache that worsens in the upright position is the clinical hallmark of CSF leaks. Treatment depends on the etiology and includes bedrest, hydration, and an autologous blood patch.

2.5. Radiologic Changes in the Brain with Normal Aging:

2.5.1. Ventricular Enlargement: *Pneumoencephalographic studies*, which allow more sharply defined measurements than do CT scans, have shown widening of the third ventricle beginning about the fourth decade [Borgersen 1966, Burhenne and Davis 1963, Engeset and Lonnum 1958, LeMay 1980]. Associated with widening of the third ventricles regression of the median part of the thalami, manifested by progressive diminution of the Massa intermedia, which, in most individuals, connects the thalami in early life. On pneumoencephalography the size and shape of the Massa intermedia has shown regression first in its posterosuperior part [LeMay 1980]. In older individuals the anterosuperior part of the massa intermedia is the last to disappear. The Massa intermedia tends to be larger throughout life in women than in men and to persist more frequently in the aging brain of women than in men. The Massa intermedia can often be seen on CT scans, but is not sharply defined and cannot be measured easily. Most pneumoencephalographic studies of the aging brain have shown a slight increase in average size of the lateral ventricles up to the seventh decade and then a more rapid increase in size [Burhenne and Davis (1963), Bruijn 1959]. Bruijn (1959) believed the measurement of the cella media (the smallest transverse diameter of the body of the lateral ventricles) gave the best correlation with the overall size of the lateral ventricles. CT studies allow less accurate measurement of the ventricles than do pneumoencephalographic studies. The margins of the ventricles are less sharply defined on CT because of partial volume

averaging and also because the shape and size of the ventricles and the skull may change due to variation in angulation of the head in the scanner [Sabattini 1982]. The photographic printouts on which measurements are often made vary at times and distort the dimensions of the skull and its contents. The effect is identical to that sometimes observed on television screens when circular objects appear elliptical. Both linear and planimetric CT measurements of the ventricles have usually been reported to show changes similar to those of pneumoencephalographic studies, that is, a statistical slight progression in size of the lateral ventricles beginning at about the fourth decade and a more striking increase after the sixth decade [Barron et.al 1976, Gyldensted 1977, Haug 1977, and Meese 1980]. The progression in size of the lateral ventricles with age is more variable than that of the third ventricle, and, as shown in neuropathology studies, many persons in the over-70-years group still have relatively small ventricles [Barron et.al 1976, Gyldensted 1977, Haug 1977, and Meese 1980].

2.5.2. Linear Ventricular Measurements: Although measurement of the ventricular span is probably more accurate on coronal than on trans axial CT [Wolpert 1977], linear measurements of the ventricles on trans axial CT and pneumoencephalography are comparable [Gawler 1976]. Ratios of the width of the ventricles to the width of the skull or brain are 'probably the most easily made and reproducible ventricular measurements on CT. **Evans ratio**, the width of the greatest span

of the frontal horns divided by the greatest width of the internal diameter of the skull, is a frequently used measurement (fig. 1). In normal individuals, even over the age of 60, Evans ratio is usually equal to or less than 0.29 (Gawler et.al 1976, Synek et.al 1976). The frontal horn ratio is the width of the frontal horns divided by the internal diameter of the skull at the same level (Hahn and Rim 1976, Pelicci et.al 1979) (fig. 1). Hahn and Rim (1976), who first described this CT ratio, examined 200 normal brains in patients and volunteers 10-81 years old. The ratio varied from 0.19 to 0.39 (mean 0.31). Except in individuals who have suffered head trauma, the lateral ventricles usually do not enlarge as much with normal aging or degenerative diseases as with hydrostatic hydrocephalus. Although early in the course of obstructive hydrocephalus the bodies of the lateral ventricles may not be large, later they often enlarge more than in individuals with hydrocephalus ex vacuo. In a study of 100 patients with obstructive hydrocephalus and 50 patients with global cerebral atrophy [LeMay and Hochberg 1979], the frontal horn ratio was found to be 0.5 or greater in 56% of the obstructive group and in only 6% of the atrophic group. The bicaudate ratio is the width of the ventricles lying between the caudate nuclei divided by the internal diameter of the skull at the same level (fig. 1). This ratio is probably more sensitive in showing change than other linear ratios and it has been used particularly in studies of children. Pelicci et al. [1979] considered ratios of 0.17 and lower to be

normal and those over 0.2 to be definitely abnormal Pelicci et al. [1979].

Banna (1977) considers the top normal bicaudate ratio to be 0.15. The cella media ratio is the narrowest width of the bodies of the lateral ventricles divided by the greatest internal diameter of the vault. Haug (1977) found a gradual increase in the mean cella media ratio with aging. In the 61-71 year range he found a mean ratio of 0.295. It was slightly larger in males than in females. Haug (1977).

The third ventricle-sylvian fissure/skull ratio is the sum of the distances between each lateral margin of the third ventricle and the ipsilateral sylvian fissure divided by the internal diameter of the skull at the same level. Brinkman (1981) found this ratio to be 0.59 or less in 77% of their demented but in only 24% of their nondemented elderly patients. Planimetric Ventricular Measurements Volumetric ratios of the ventricles have been studied by measuring the size of the lateral ventricles with a planimeter [Barron et.al 1976] or using a grid method (Benes et.al 1982) and dividing it by the total area of the brain within the CT scan cut. The areas are presumed to be related to the volumes and therefore reflect the size of the ventricles. The measurements are usually made on one or two slices, and the anatomic areas measured may vary in different individuals depending partly on the shape of the head and its angulation in the scanner. Reproducible measurements are more difficult when the

ventricles are small. Volumetric Measurements of Cerebrospinal Fluid (CSF) Intracranial Space. (Benes et.al 1982).

On CT scans of 130 individuals without localized disease, Ito et al. (Ito et.al 1981) estimated the volume of the brain, CSF (ventricles), and cranial cavity by counting the number of pixels in each tissue on scans taken through the hemispheres. They found the mean CSF volume to increase progressively after the age of 40 years. (Zatz et.al 1982) studied the volume of intracranial fluid in 123 normal subjects 23-88 years old using semi-automated computer analysis, and found a marked individual variation in the older patients but relatively little increase in the volumes until the seventh decade. (Zatz et.al 1982)

2.5.3. Fissural and Sulcal Enlargement: As has been found in neuropathologic studies, involutory changes in the temporal lobes with widening of the anterior ends of the sylvian fissures is one of the earliest changes seen on CT in the aging brain. In CT studies the anterior end of the left sylvian fissure is more frequently wider than the right, which correlates with the findings of von Braunmuhl et.al (1957), who found greater atrophic changes with aging in the anterior left temporal lobe than in the right on pathologic study. Widening of superficial sulci also occurs with aging and has been described on pathologic studies, particularly in the parasagittal sulci of the frontal and parietal lobes [von Braunmuhl et.al (1957), Tomlinson et.al (1968), Hooper and Vogel (1976). On CT scans widening of the interhemispheric fissure is commonly seen anteriorly extending back to, and

occasionally just beyond, the callosomarginal sulci, which commonly enlarge, but widening of the fissure more posteriorly is seen much less often. Cala et.al (1982), studying sulcal widening on CT scans of 115 healthy volunteers 14-40 years old, found progressive sulcal widening, mainly in the frontal lobes and the cerebellar vermis, starting in the teens. Although there is statistically some progressive enlargement of the third and lateral ventricles and superficial sulci with age, there is often poor correlation between ventricular size and superficial sulcal widening (Gyldensted 1977); this suggests these atrophic changes may be independent of each other.

When the superficial sulci are widened over the hemispheres, the main sulci (central, pre- and postcentral, and superior frontal), which are formed early in the developing brain, are deep, and when widened are seen on CT more clearly than on inspection of the brain surface [kido et.al 1980]. Widening of superficial sulci seen with aging is often described in radiologic literature as "cortical atrophy," but this is probably misleading, and "gyral atrophy" or "superficial atrophy" seems preferable. As noted before, neuropathologic studies have shown no statistically significant narrowing of the cerebral cortex with aging. [kido et.al 1980]

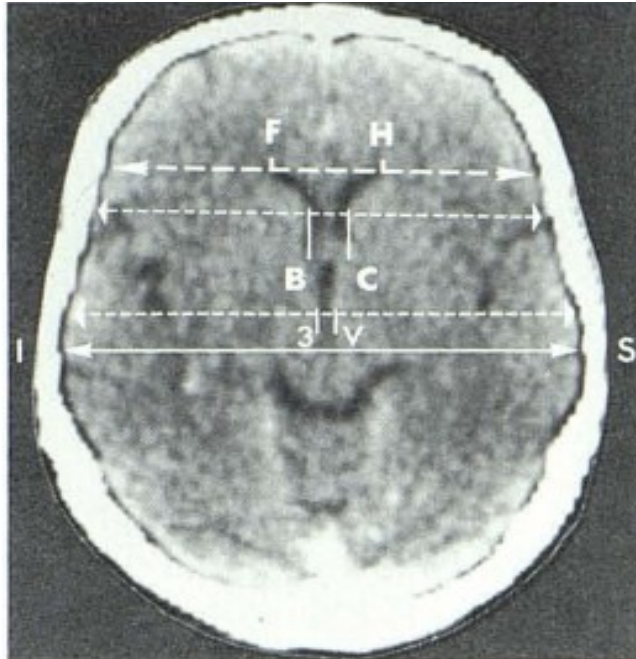


Fig. 1.-Linear ratios used in ventricular measurements.

Frontal horn ratio = width of frontal horns (FH)/internal diameter of vault at same level; bicaudate ratio = width of ventricles between caudate nuclei (BC)/internal diameter of vault at same level; third ventricular ratio = greatest width of third ventricle (3V)/ internal diameter of vault at same level; Evans ratio = width of frontal horns/greatest internal diameter of "ault (IS).

2.6. Previous Study:

2.6.1. Mortazavi et.al 2013, study the ventricular system of the brain: a comprehensive review of its history, anatomy, histology, embryology, and surgical considerations

The cerebral ventricles have been recognized since ancient medical history. Their true function started to be realized more than a thousand years later. Their anatomy and function are extremely important in the neurosurgical panorama. His method based on the literature that was searched for articles and textbooks of different topics related to the history, anatomy, physiology, histology, embryology and surgical considerations of the brain ventricles. He concludes that; Herein, we summarize the literature about the cerebral ventricular system.

2.6.2. Prince 2012, was aimed to establish the range of the sizes for the different parts of the cerebral ventricular system. These simple measurements should be applicable to the brain Computed Tomography Scan reading without any need for advanced morphometric software package. Three hundred (150 females and 150 males) normal brain CT scans were obtained from a private Diagnostic Radiology center in Harare for ventricular dimensions' measurements (bi frontal, third ventricular and fourth ventricular dimensions). 18 hydrocephalus patients were also included in the study. A MILLENSYS DICOM Viewer Version 9® USA software program was used to measure ventricular dimensions in millimeters. his study found an average

(Mean±SE) frontal horn diameter, third ventricle width, fourth ventricle width, fourth ventricle height, Frontal Horn ratio (A/B), and the third ventricle ratio (C/D) for the sample being $31.8\pm 0.2\text{mm}$, $3.25\pm 0.09\text{mm}$, $10.6\pm 0.1\text{mm}$, 10.5 ± 0.1 , 0.313 ± 0.002 , and 0.030 ± 0.002 , respectively. Except for the fourth height which was not significantly affected by age ($p=0.515$), the present study showed that there was a significant difference between different age groups on all of the above measurements and ratios ($p<0.01$). Criteria have been developed that are measurable, reproducible and applicable in routine diagnosis of dilated cerebral ventricles in adults. In general, the maximum frontal tips diameter greater than 48% or less than 25% corresponding plane are to be considered highly suspicious of abnormal ventricles. The overall frontal horn ratio of the eighteen hydrocephalus patients varied from 0.36 to 0.52 with an overall mean of 0.42.

2.6.3. Gameraddin et.al (2015) stated that as ageing advances, the human brain undergoes many gross and histopathological changes with regression of the brain tissue leading to the enlargement of the ventricles. Knowledge of morphometric and size of normal ventricular system of brain is important to understand these changes. Methods: For the present perspective study, computerized tomography(CT) for 152 patients (Males—89 and Females—63) were studied for the measurements of fourth ventricle, third ventricle and lateral ventricle and it was statistically analyzed. Results: The anteroposterior extent of the

body of the lateral ventricles on the right side was 74.89 ± 9.86 mm and 70.06 ± 8.83 mm in the males and females and on the left side was 74.89 ± 9.89 mm and 69.56 ± 11.42 mm in the males and females; the length of the frontal horns on the right side was 28.53 ± 3.88 mm and 26.16 ± 4.21 mm in the males and females and on the left side was 28.53 ± 3.88 mm and 26.17 ± 4.237 mm in the males and females respectively. The width and height of the fourth ventricle were 12.54 ± 1.90 mm and 9.66 ± 2.12 in the males and 11.60 ± 2.099 mm and 9.70 ± 2.219 in the females respectively. The width of the third ventricle was 5.70 ± 1.54 mm and 5.40 ± 1.68 mm in the males and females respectively. Conclusion: The present study has defined the morphometric measurements of the lateral ventricles, third ventricle, and fourth ventricle of the brain which has clinical correlations in diagnosis and for further line of treatment.

2.6.4. Adams and Wilson (2011) stated that the inherent spatial complexity of the human cerebral ventricular system, coupled with its deep position within the brain, poses a problem for conceptualizing its anatomy. Cadaveric dissection, while considered the gold standard of anatomical learning, may be inadequate for learning the anatomy of the cerebral ventricular system; even with intricate dissection, ventricular structures remain difficult to observe. Three-dimensional (3D) computer reconstruction of the ventricular system offers a solution to this problem. This study aims to create an accurate 3D computer reconstruction of the ventricular system with surrounding

structures, including the brain and cerebellum, using commercially available 3D rendering software. Magnetic resonance imaging (MRI) scans of a male cadaver were segmented using both semiautomatic and manual tools. Segmentation involves separating voxels of different grayscale values to highlight specific neural structures. User controls enable adding or removing of structures, altering their opacity, and making cross-sectional slices through the model to highlight inner structures. Complex physiologic concepts, such as the flow of cerebrospinal fluid, are also shown using the 3D model of the ventricular system through a video animation. The model can be projected stereoscopically, to increase depth perception and to emphasize spatial relationships between anatomical structures. This model is suited for both self-directed learning and classroom teaching of the 3D anatomical structure and spatial orientation of the ventricles, their connections, and their relation to adjacent neural and skeletal structures.

2.6.5. Mangesh et.al 2014, stated that the structure of human brain is complicated and not yet fully understood. As the human brain ages, characteristic structural changes occur that are considered normal. Thus the thorough knowledge of the normal changes that occur in the brain with age is critical before abnormal findings are analyzed. The normal ventricular size during life was previously unknown. In the past pneumo-encephalogram was the most valuable test for determining ventricular size during life, but this method was not practical due

to discomfort and morbidity. Advances in sophisticated and sensitive imaging techniques like the computerized tomography scan helps in dramatic expansion of our understanding of the normal structure of brain without the use of contrast media as well as it helps to understand the changes taking place in brain in normal individuals. CT scan provided a revolutionary means for morphologic study of the brain in vivo. The first purpose of this study was to examine the different dimensions of fourth ventricle. Many studies report a strong relationship between age and different measures of ventricular system. The study was carried out in adult individuals with age group 20-60 years and in ageing individuals above 60 years.

2.6.6. Singh et.al (2014), stated that as the human brain ages, characteristic structural changes occur that are considered to be normal and are expected. Thus the thorough knowledge of the age related normal changes that occur in the brain is required before any abnormal findings are analyzed. As ageing advances, the brain undergoes many gross and histopathological changes with regression of the brain tissue leading to the enlargement of the ventricles. To understand these changes the knowledge of normal morphometry and size of normal ventricular system of brain is important. **Materials & Methods:** For the present study 358 (Males - 207 and Females - 151) individuals Computerized Tomography (CT) images of brain studied. Measurements of fourth ventricle, third ventricle and lateral ventricle were noted down from CT images and it was statistically analyzed. **Results:** After

analysis it was observed that the height and width of the fourth ventricle was larger in males as compared to females. The length of the third ventricle was observed to be greater in females than in males. The width of the third ventricle it was observed to be greater in males than in females. Antero-posterior extent of the left frontal horn (males = 26.26 ± 2.94 , 95% CI 25.86 - 26.66 mm and females = 26.53 ± 3.38 , 95% CI 25.99 - 27.08 mm) was greater than that of the right ones (males = 25.00 ± 3.18 , 95% CI 24.57 - 25.44 mm and females = 25.34 ± 3.50 , 95% CI 24.78 - 25.90 mm). Conclusion: Advances in sensitive imaging techniques like the Computerized Tomography helps in dramatic expansion of our understanding of the normal structure of brain. The present study has defined the morphometric measurements of the lateral ventricles, third ventricle, and fourth ventricle of the brain which has clinical correlations in diagnosis and for further line of treatment.

2.6.7. Parija et.al (2016) aimed to find out age-related changes in ventricular system of brain in normal individuals from younger to elderly groups in both sexes. Methods: Sixty normal females and males within ages, 15 to 70 years were examined by computed tomography (CT) scan of brains. Measurements of lateral, third and fourth ventricles were considered by arranging the subjects into 3 age-groups, 15 to 30, 31 to 50 and 51 to 70 years. After taking due measurements, Schaltenbrand index was calculated. Results: Size of all ventricles had insignificant increase or no change from the youngest (15 to 30 years) to the middle age-

group (31 to 50 years), but the width of third ventricle was found to increase in most males and females in the elderly group. Males had higher values of enlargement than females in all ventricles. Measurements of AP length of frontal horn and frontal horn with body remained almost constant in the youngest age-group, which increased with ageing. Schaltenbrand index values decreased steadily from younger to higher age-groups. Conclusion: Sizes of all three ventricles were more in elderly individuals. In both higher age-groups, males had more expansion of ventricular system than females. Increase in ventricular size was more evident in the lateral ventricle. Changes in ventricular size did not show any effective change in cranial diameters.

Chapter Three

Methodology

3.1. Materials:

The study executed using magnetic resonance imaging scanner; called Signa HDxt 1.5T provides with advanced technology, such as: A proven, homogeneous 1.5T magnet delivering a full 48cm field of view. 16-channel RF. HD gradients engineered for high-fidelity to produce high accuracy waveforms. HD Reconstruction engineered for real-time, high-performance image generation. Advanced, high-definition applications such as Cube and IDEAL that help deliver images with premium quality and clarity. High-Density coils engineered with coil elements that are optimized for

the anatomy and exam. GE Signa HDx 1.5T Technical Specifications; magnet: 1.5 Tesla, Superconducting, Clinical Application: Whole Body, Configuration: Compact Short Bore, Power Requirements: 480 or 380/415, Cooling System: Closed-loop water-cooled gradient, Cryogen Use: Less than 0.03 L/hr. liquid helium, Spectroscopy: Possible, Synchronization: ECG/peripheral, respiratory gating, (Smart Prep, Smart Step), Pulse Sequences (Standard): SE, IR, 2D/3D GRE and SPGR, Angiography: 2D/3D TOF, 2D/3D Phase Contrast; 2D/3D FSE, 2D/3D FGRE and FSPGR, SSFP, FLAIR, EPI, Pulse Sequences (Optional): 2D/3D Fiesta, FGRET, Spiral, Tensor, imaging Modes: 2D single slice, multi slice, and 3D volume images, multi slab, cine, FOV: 1cm to 48cm continuous, Slice Thickness: 2D 0.7mm to 20mm; 3D 0.1mm to 5mm, Display Matrix: 1028 x 1024, Measuring Matrix: 128 x 512 steps 32 phase encode and Pixel Intensity 256 gray levels, Also MDCT machine with 64-slice, detector array, fan beam shape, CT monitor in case of comparison of this study finding with that reported in CT literature.



Fig. (3.1) GE Signa HDx 1.5T

3.2. Methods:

3.2.1. Technique:

The patient under examination must perform MRI brain the technique performed to normal brain anatomy; *Axial T2-W FLAIR*. FLAIR is a similar sequence to STIR but in this case it uses a longer inversion time (approximately 2200ms) to suppress CSF and increase conspicuity of the lesion. The axial plane is useful as it is comparable to CT (TE/TR/TI = 148 /9200ms /2200ms FOV = 22-25cm, Slice thickness/gap = 5/1mm). Axial T2 weighted images, also the flair axial T2, axial T1, coronal T2 and T1 AXIAL, all these sequences were performed in brain scan and then the

ventricular measurement were done in correspondence sections as:

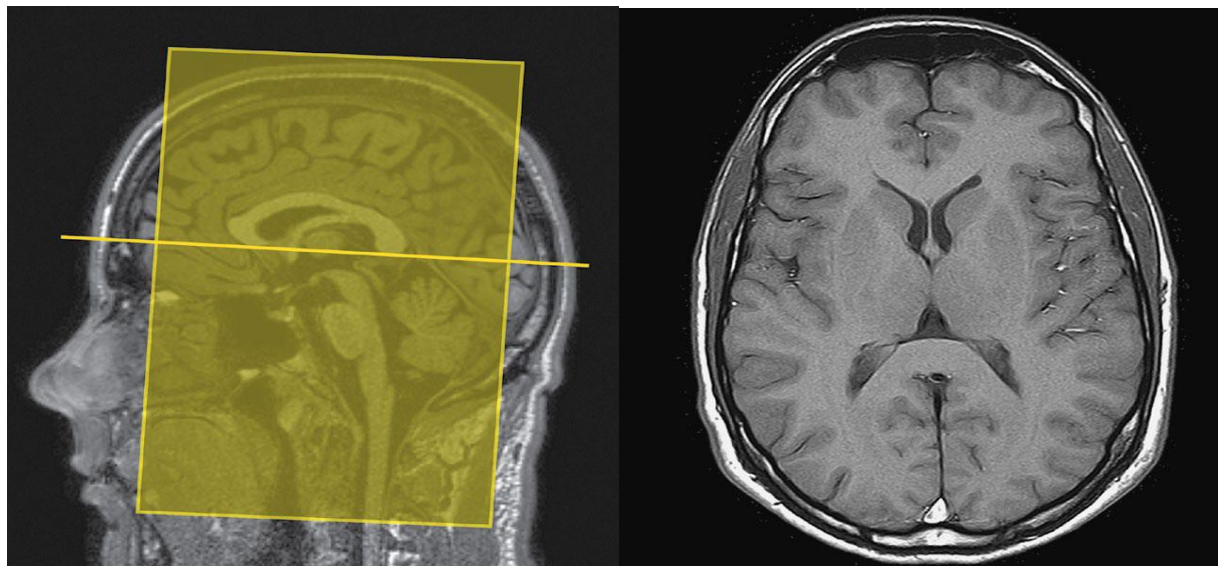


Fig. (3.2) Axial IR T1-weighted image using a TI of 700ms with the level of the cuts demonstrated in sagittal T1 weighted images (left)

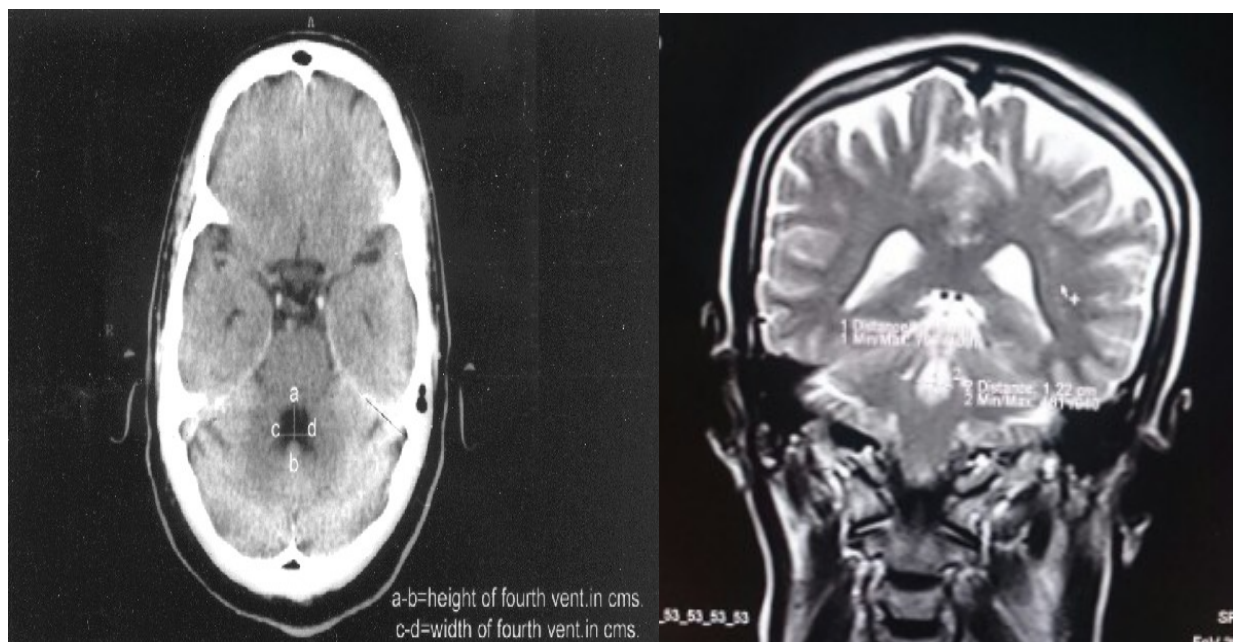


Fig.3.3. Level of fourth ventricles measured at coronal section (right) in our study left image as standard where the measurement is based

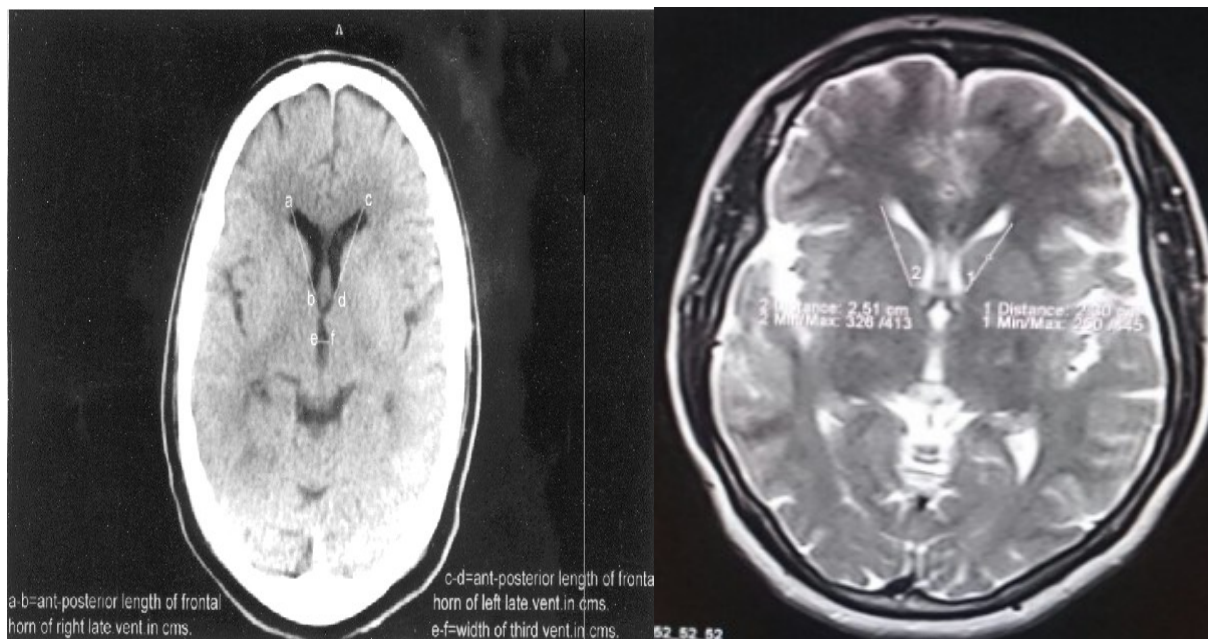


Fig. 3.4. Level of interventricular foramen showed horns measurement

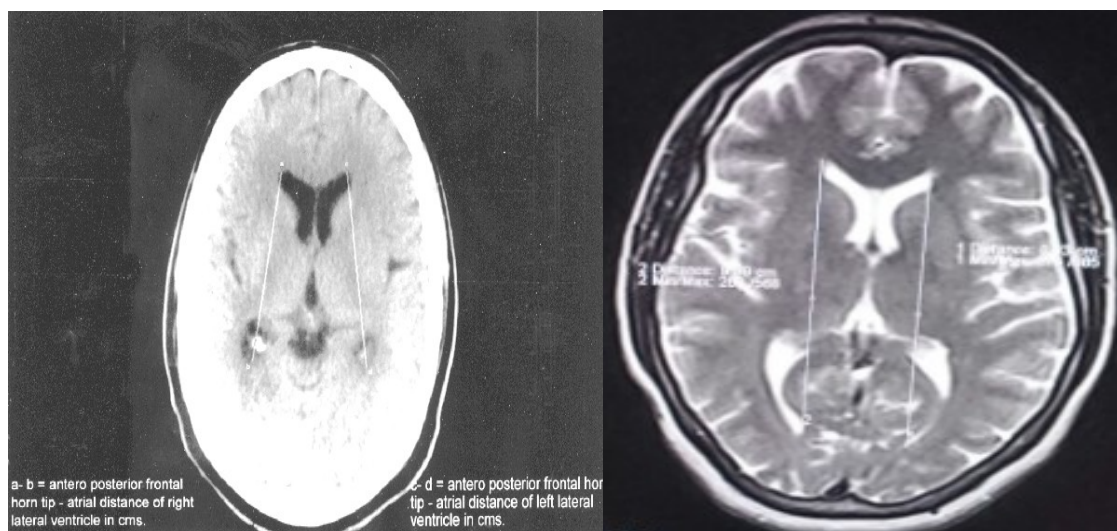


Fig.3.5. Level above the interventricular foramen showed our length of lateral ventricular measures in Right image (axial MRI)

3.2.2. Study Design:

An analytical case control study used to measure the brain ventricular system in MRI images.

3.2.3. Study Sample:

The study sample was consisted of 60 patients with normal brain MRI scan.

3.2.4. Area of the Study:

This study conducted at Khartoum state hospitals, diagnostic centers

3.2.5. Duration of the study:

This study conducted in period from January 2016 May 2016.

3.2.6. Population of the Study:

The population of this study was data set (brain MR Images), where the brain was free from disease. The study includes both gender with their age ranged from one years to ten years old for child patient, 14-65 for female and 19-65 for male population.

3.2.7. Inclusion Criteria:

All patients with normal brain MRI scan, no pathological abnormalities were included.

3.2.8. Exclusion Criteria:

All patients with abnormal brain MRI scan were excluded from this study especially the disease affected the ventricular size.

3.2.9. Method of data analysis and presentation:

All data were presented as mean± SD values. Data were analyzed by correlation analysis with the use of the SPSS (Inc., Chicago, Illinois version 16) and excel Microsoft office 2013. A value of $P < 0.05$ was considered significant.

3.2.10. Data collection variables:

Patient gender, Age, weight, History of complication, RVL, LVL, RVW, LVW, RA-PL, LA-PL, RAL, LAL, FVL, FVW, ADW, TVW, and BPD.

3.2.11. Ethical considerations:

- There was official written permission to Khartoum state diagnostic centers to take the data.
 - No patient data were published also the data was kept in personal computer with personal password.

Chapter four

Table 4.1 showed mean STD for the ventricular measurement according to the gender including age and patient weight

Parameters	Female	Male	Child
Age	33.48±17	38.2±13.8	5.1±2.6
Wight	67.52±11.1	71.3±9.0	19.7±9.1
LVL	5.3±0.96	6.0±0.79	5.49±0.71
LVW	1.4±0.19	1.56±0.4	1.09±0.19
RVW	1.3±0.20	1.5±0.27	1.02±0.26
RVL	5.4±0.82517	5.9±0.69	5.3±0.57
ADW	0.26±0.07	0.29±0.05	0.25±0.041
FVW	1.392±0.19	1.59±0.24	1.35±0.42
FVL	1.05±0.27	0.9±0.32	0.8431±0.26
RA-PL	8.07±0.9	8.4±0.84	7.4±0.35
LA-PL	8.16±1.0	8.6±1.04	7.3238±0.34
LAL	2.48±0.24	2.6±0.19	2.18±0.29

RAL	2.49±0.17	2.6±0.19	2.23±0.26
TVW	0.29±0.06	0.3±0.07	0.2±0.06
BPD	12.19±0.47	12.9±0.5	12.02±0.69

Figure (4.1) showed the age difference between the three classes of study including gender and age of the child.

Figure (4.2) correlation between the Left lateral ventricular widths with Aqua duct widths in children

Figure (4.3) correlation between the RT lateral ventricular widths with AD widths in children

Figure (4.4) correlation between third ventricle widths with AD widths in children

Figure (4.5) correlation between the Left lateral ventricular widths with AD widths in male population

Figure (4.6) correlation between the RT lateral ventricular widths with AD widths in male

Figure (4.7) correlation between the third ventricle widths with AD widths in male

Figure (4.8) Correlation between the lateral ventricular width and length

Figure (4.9) correlation between the right ventricular width and lateral ventricular width.

Figure (4.10) correlation between the right lateral ventricular length and patient age

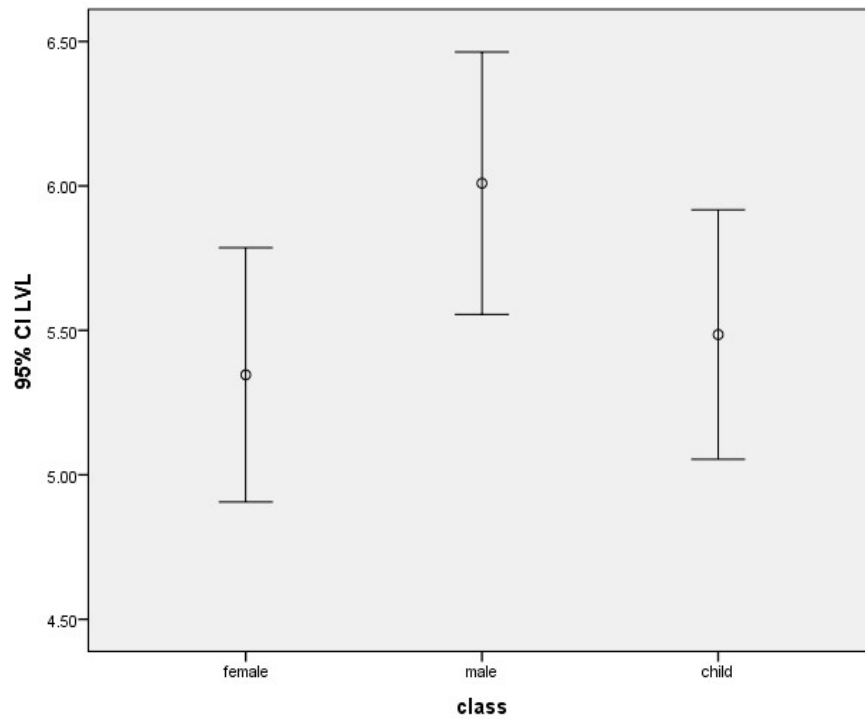


Figure (4.11) simple error bar showed the difference in lateral ventricular length between the male female, and children.

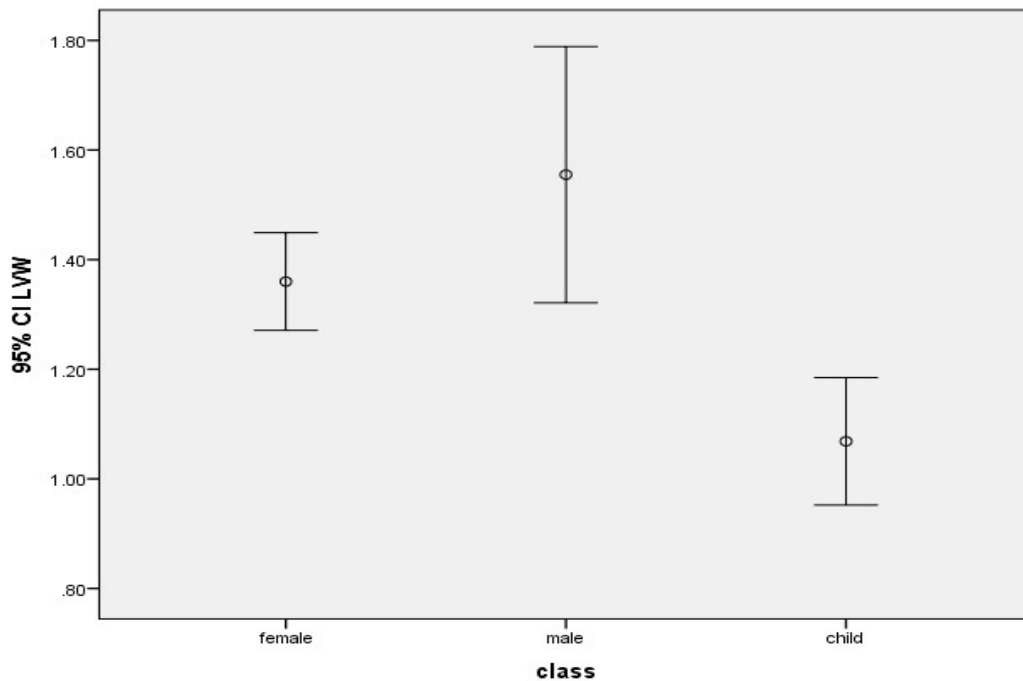


Figure (4.12) simple error bar showed the difference in lateral ventricular width between the male female, and children

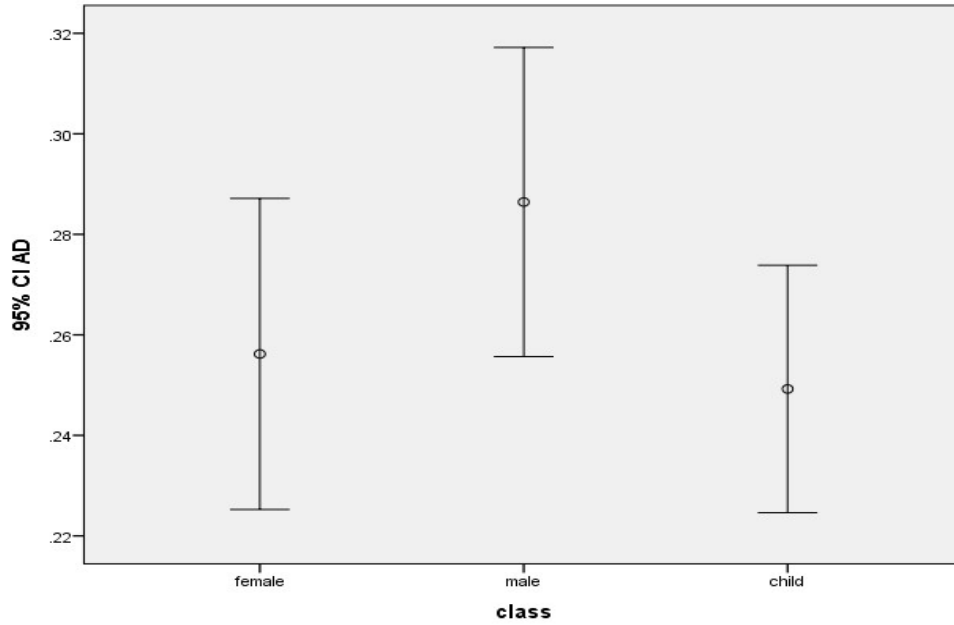


Figure (4.13) simple error bar showed the difference in AD width between the male, female, and children

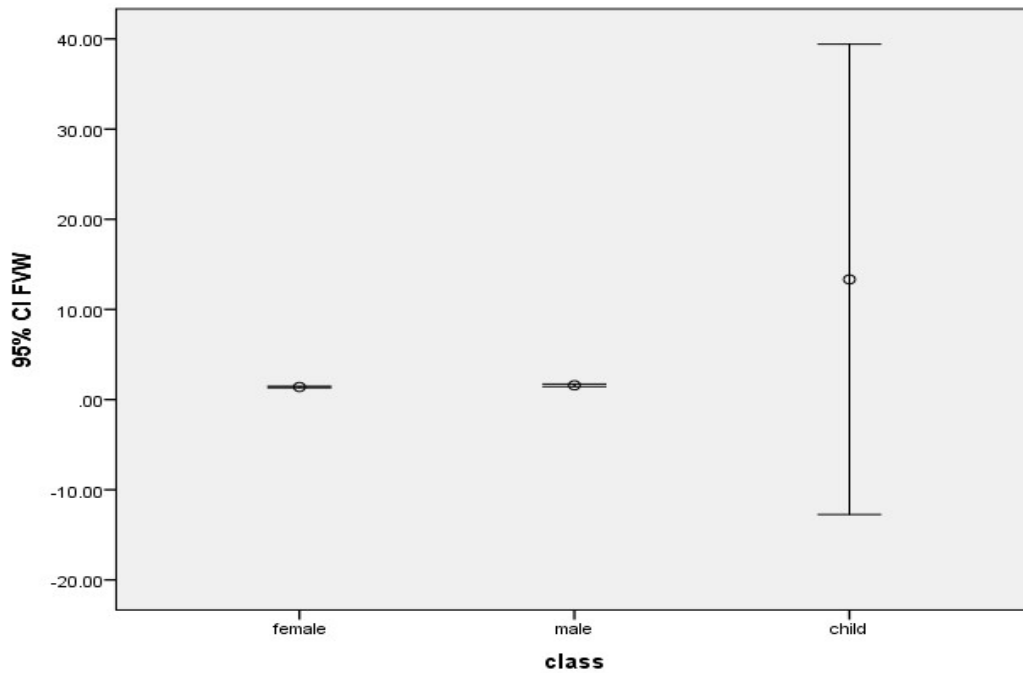


Figure (4.14) simple error bar showed the difference in fourth ventricle width between the male female, and children

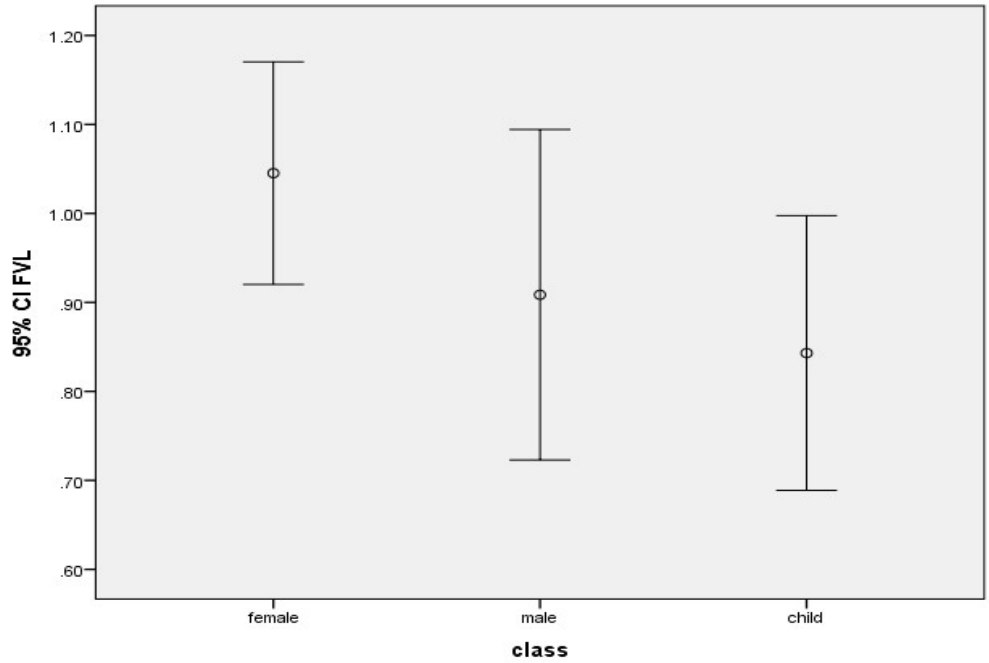


Figure (4.15) simple error bar showed the difference in fourth ventricular length between the male female, and children

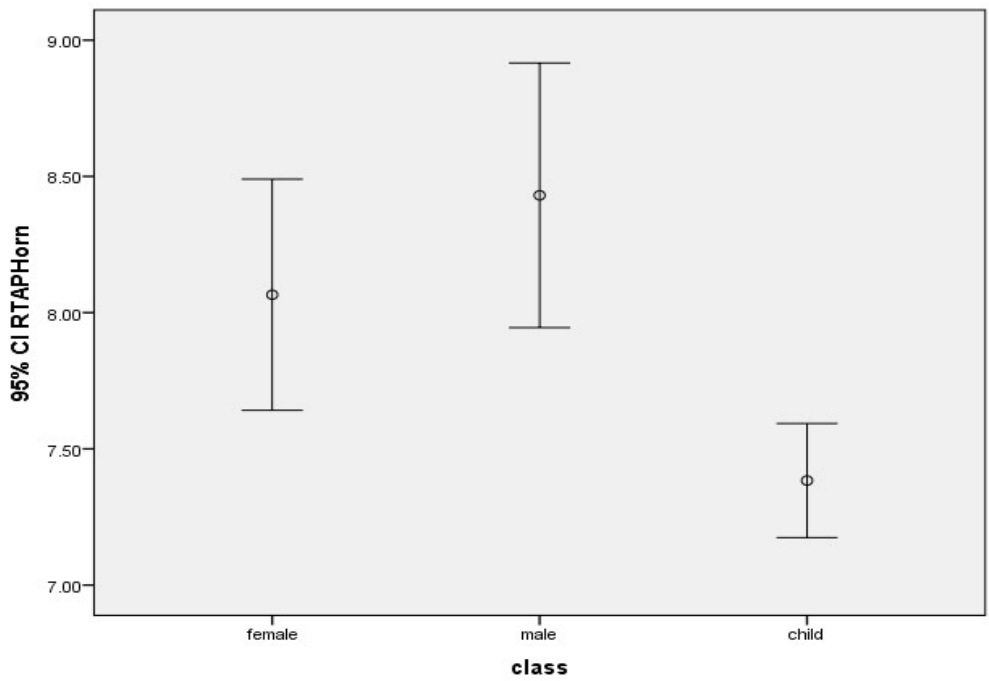


Figure (4.16) simple error bar showed the difference in RT ANT horn of lateral ventricle between the male female, and children

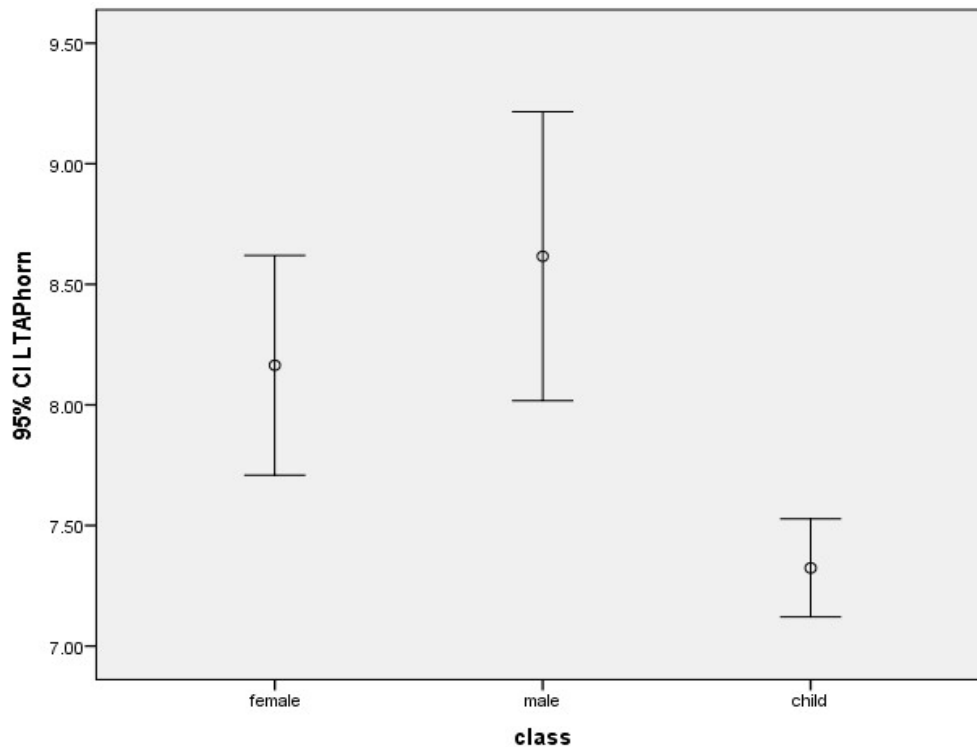


Figure (4.17) simple error bar showed the difference in LT ANT horn of lateral ventricle between the male female, and children

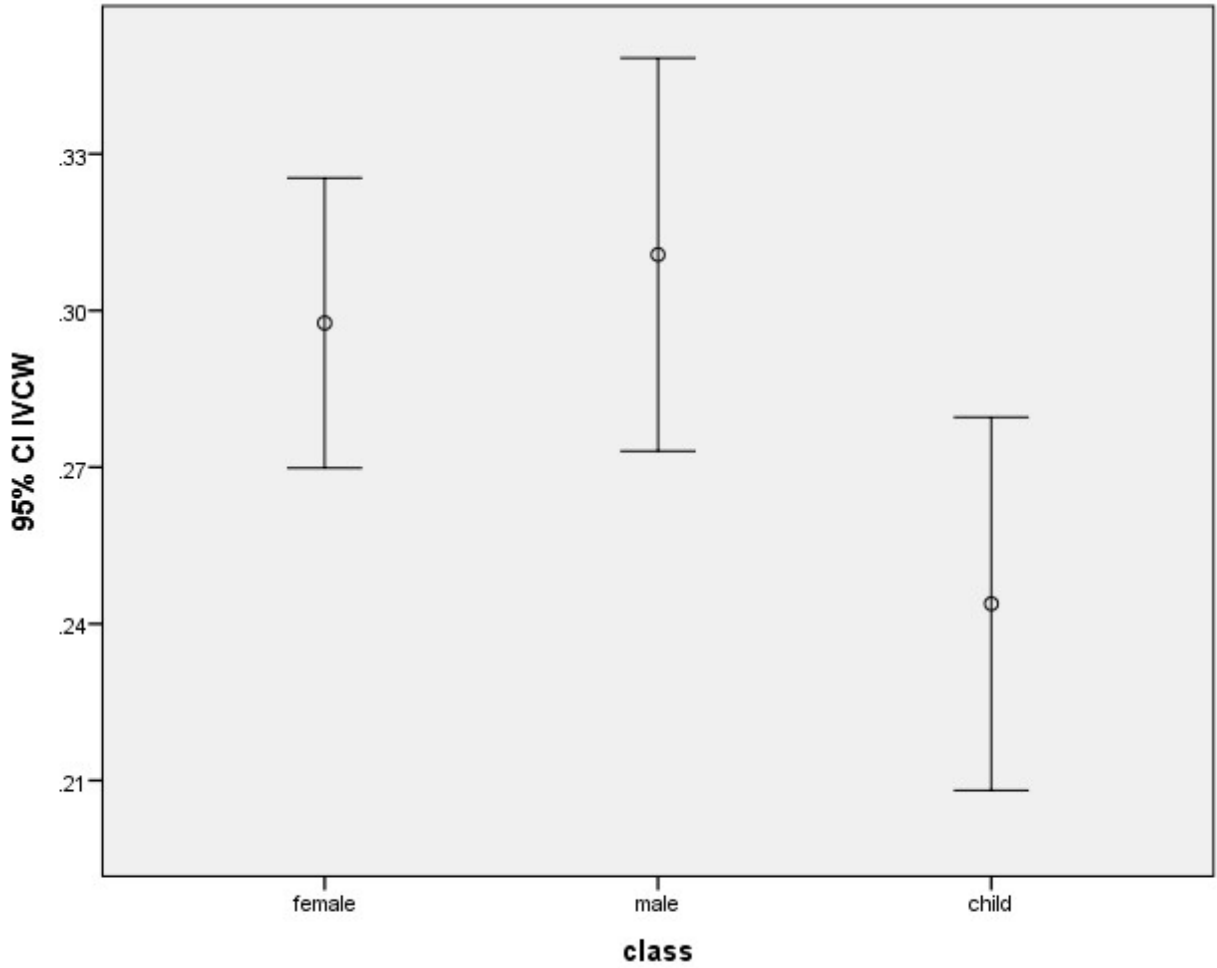


Figure (4.18) simple error bar showed the difference in interventricular canal between the male female, and children

Chapter Five

Discussion, Conclusion and Recommendations

5.1. Discussion:

The human nervous system is the most complex, widely investigated and yet poorly understood physical system known to mankind (williams et.al 1995). Studies by Ellis (1920), Pakkenberg and Volgt et.al (1976) and Kaban and Sadowsky (1978) revealed that brain regression involving both the cerebrum and the cerebellum usually began by the seventh decade and thereafter accelerated with advancing age. This study was intended to measure and establish the reference measurement for brain ventricular system in MRI for three group of Sudanese population male, female and children under age of 15 years. Age, Wight of the patient, left Lateral Ventricle Length, left lateral Ventricular Width, right Ventricular Width, Right Ventricular Length, Aqua Ductal width, Fourth Ventricular Width, Fourth Ventricular length, right Antero-posterior Horn length, Left Antero-posterior horn, left Anterior Horn length, right Anterior horn length, third ventricle width and BPD. Which having the mean value described as follow: One of the most important factor that affect these measurements were age distribution of all three class under study and the collected data revealed higher age of male rather than female populations of the study, as described in figure (4.1). Measurement of lateral ventricles length above to the inter ventricular foramen measured from the most anterior part of the

frontal horn to the most posterior part of occipital horn for right and left lateral ventricles in axial T2 weighted image for male and female and child, the mean value for the right anterior to posterior horn for this group for male (8.4 ± 0.84), female (8.07 ± 0.9) and child (7.4 ± 0.35), the mean value for the left anterior to posterior horn for male (8.6 ± 1.04), female (8.16 ± 1.0) and child (7.3238 ± 0.34). Table (4-1).

Measurement of the length of frontal horn at the level of interventricular foramen for right and left horn in axial T2 weighted image for male and female and child, the mean value for right frontal horn for male (2.6 ± 0.19), female (2.49 ± 0.17) and child (2.23 ± 0.26), the mean value for left frontal horn for male (2.6 ± 0.19), female (2.48 ± 0.24) and child (2.18 ± 0.29), According to Glydensted (1977), Gomori et.al (1984) Takeda and Matsuzawa (1985) and Goldstein et.al (2001) the left lateral ventricle was larger than the right one and both were larger in males. In our study, the anteroposterior extent of the left frontal horns for males (2.6 ± 0.19) and females (2.48 ± 0.24) was symmetrically in right frontal horn for males (2.6 ± 0.19) and mildly lesser than that of right frontal horn for females (2.49 ± 0.17). The anteroposterior extent of the left lateral ventricular bodies including their frontal horns for male (8.6 ± 1.04) and females (8.16 ± 1.0) was greater than the right one's male (8.4 ± 0.84) and females (8.07 ± 0.9)

Measurement of bi parietal distance in the region above to the interventricular foramen at the brain midpoint from inner most layer of skull to the inner most layer in opposite side in axial T2

weighted image for male, female and child, the mean value for (12.9±0.5cm), (12.19±0.47cm), and (12.02±0.69cm) respectively, this value was measured in order to calculate the ratio between the brain volume and the ventricular size which equal to (1:10) when choosing the onside ventricular width.

Also Measurement of width of third ventricle in axial T2 weighted image for male, female and child, the mean value for male (0.3±0.07cm), female (0.29±0.06cm) and child (0.2±0.06cm) according to Gawler et.al (1976), Brinkman et.al (1981) and Soininen et.al (1982) found that the maximum width of the third ventricle had a mean of 0.46 cms, 0.59 cms and 0.92+2.71 respectively. With higher values in males. In our present study we recorded this measure significantly higher in males (0.3±0.07cm) as compared to female (0.29±0.06cm) table 4.1.

the width of lateral ventricles measure at most widest and highest region and measure the length in the same region in the right and left ventricles in axial T2 weighted image for male, female and child, the mean value for right ventricles width for male was (1.5±0.27cm) and length in same region (5.9±0.69cm), female (1.3±0.20cm) and length in same region (5.4±0.83 cm) and child (1.02±0.26) and length in same region (5.3±0.57cm), the mean value for left ventricles width for male was (1.56±0.4cm) and length in same region (6.0±0.79cm), female (1.4±0.19cm) and length in same region (5.3±0.96cm) and child (1.09±0.19cm) and length in same region (5.49±0.71cm).

Fourth ventricles length and width in coronal T2 weighted image for male, female and child, the mean value for length of fourth ventricles was $(0.9 \pm 0.32 \text{ cm})$, $(1.05 \pm 0.27 \text{ cm})$ and (0.8431 ± 0.26) respectively. The mean value for width of fourth ventricles was $(1.59 \pm 0.24 \text{ cm})$, (1.392 ± 0.19) and $(13.3 \pm 43.17 \text{ cm})$ respectively. Studies by Galwer et.al (1976) revealed that the greatest distance between the roof and floor of the fourth ventricle was less than 1.2 cms with a mean of 1.08 cms; however, in this study the distance is significantly higher in female than male group which was the only one value noted to be bigger in female.

Measurement of anterior to posterior distance of aqua duct in the region midway between third and fourth ventricles in sagittal T1 weighted image for male, female and child was done in order to assess the size of this canal and furthermore testing the effect of this canal on the other ventricular measurement, the mean value of this distance was (0.29 ± 0.05) , (0.26 ± 0.07) and (0.25 ± 0.041) . This study also concerns with investigation of effect of aqua duct dimensions in lateral ventricles width and other measurement, a correlation was done between AD width and LVW, a direct linear correlation noted when AD width increased by one unit in child samples the width of Left Ventricle increased by (5.7669 mm) Figure (4.2), and when AD increased by one unit the width of right ventricles increased by (3.8901 mm) Figure (4.3), and when AD increased by one unit the width of interventricular foramen increased by (0.9401 mm) Figure (4.4) the correlations co-efficient for these values and linear equations are

$(y=5.7669x-0.3422)$ ($R^2 = 0.8179$), $(y=3.8901x+0.0669)$ ($R^2=0.2281$), $(y=0.9401x+0.0139)$ ($R^2 = 0.2304$) respectively.

A direct significant linear correlation noted when AD width increased by one mm in male samples the width of left ventricle increased by (1.7673mm) **$(y = 1.7673x+0.9955)$, ($R^2 = 0.0733$) as showed in** Figure (4.5), when AD width increased by one (mm) the width of right ventricle increased by (1.8762mm) Figure (4.6), when AD width increased by one unit the width of interventricular foramen increased by (0.5047) Figure (4.7).

According to Taveras and Wood (1976) the lateral ventricular contours are relatively constant. Except for the occipital horns. Alteration in the brain with aging have been the focus of many investigations. According to Fox et.al (1975) Huckman et.al (1975) Roberts and Caird (1976) LeMay (1984) and Lee and Krishna (1987), modern computerized x-ray tomography allows easy and safe noninvasive study of the ventricular system, without complication, so unlike the pneumoencephalogram and it can be used as a screening procedure for many illnesses. Roberts et.al (1978) pointed out its value in evaluation dementia and its use in excluding brain diseases that mimic dementia of the Alzheimer type such as neoplasms, subdural hematomas and cerebrovascular disease. The range of changes in the ventricular size of the brain encountered in clinical practice can lead most people to believe that a decision taken without an exact measure of ventricular size, however. There is likely to be an increasing

number of circumstances in which precise measurements will be of value.

5.2. Conclusion

The present study defined the morphometric measurement of all ventricles of the brain i.e. the fourth ventricle, third ventricle and lateral ventricle, which has clinical correlations in diagnosis, treatment and surgical intervention. Where the general aims of this study was to calculate the brain ventricular measurement in magnetic resonance images using normal MRI caliber in order to establish a reference base for brain ventricles in Sudanese populations also to compare between these measurements in three different classes. 60 patients with normal MRI brain scan (or clinical indication that not affect the ventricular system) with slice thickness range from 3-5 mm was performed in both Antalya diagnostic center and Nilein medical diagnostic center in period from September 2015- until April 2016. The measurement was performed for Age, Weight of the patient, left Lateral Ventricle Length, left lateral Ventricular Width, right Ventricular Width, Right Ventricular Length, Aqua Duct, Fourth Ventricular Width, Fourth Ventricular length, right Antero-posterior Horn length, Left Antero-posterior horn length, left Anterior Horn length, right Anterior horn length, third ventricle width and BPD. And the mean values for these measure was (33.48yers, 67.52kg, 5.3, 1.4, 1.3, 5.4, 0.26, 1.392, 1.05, 8.07, 8.16, 2.48, 2.49, 0.29 and 12.19 cm) for female patients, (38.2yrs, 71.3 kg, 6.0, 1.56, 1.5, 5.9, 0.29, 1.59, 0.9, 8.4, 8.6, 2.6, 2.6, 0.3 and 12.9cm) for male patient and 5.1yrs, 19.7kg, 5.49, 1.09, 1.02, 5.3, 0.25, 13.3, 0.8431, 7.4, 7.3238, 2.18, 2.23, 0.2, and 12.02cm) for child under age of 15years respectively. The

correlation reveal that direct significant correlation between the Aqua Duct and the ventricular width and interventricular canal as mentioned in discussion section also all measurement were higher in male than female in which both higher than child patient.

5.3. Recommendations:

- More data is required for future scope in this field of research in order to represent the measurement more efficiently.
- The introduction of magnetic resonance images in measuring of brain ventricular system dimensions is consider on of the important parameters in this research so the study recommends to use this MRI rather than CT with small slice thickness with consistent level of cuts to measure the brain ventricle.
- This study recommends to evaluate this measurement by volume study for more accuracy.

References:

- Aitken AR (1996) A ventricular catheter guide for rapid and accurate ventricular access. *J Clin Neurosci: Off J Neurosurg Soc Australasia* 3:257-260
- Banna M. The ventriculo-cephalic ratio on computed tomography. *J Can Assoc Radio/1977; 28:208-210*
- Barron SA, Jacobs L, Kinkel WR. Change in size of normal lateral ventricles during aging determined by computerized tomography. *Neurology (NY)* 1976;26: 11 01-1113
- Benes F, Sunderland P, Jones BD, LeMay M, Cohen BM, Lipinski JF. Normal ventricles in young schizophrenics. *Br J Psychiatry* 1982;141 :90-93
- Bhagwati S (1964) A case of unilateral hydrocephalus secondary to occlusion of one foramen of Monro. *J Neurosurg* 21:226-229
- Bickers DS, Adams RD (1949) Hereditary stenosis of the aqueduct of Sylvius as a cause of congenital hydrocephalus. *Brain* 72:246-262
- Blatt ES, Berkmen YM (1969) Congenital occlusion of the foramen of Monro. *Radiology* 92:1061-1064
- Borgersen D. Width of the third ventricle. *Acta Radiol (Stockh)* 1966;4: 645-661
- Brinkman SD, Sarwar M, Levin H, Morris HH III. Quantitative indexes of computed tomography in dementia and normal aging. *Radiology* 1981; 138: 89-92
- Broman I (1927) Människans utveckling före födelsen: En kortfattad handledning i människans embryologi. Gleerup, Lund
- Bruijn JW. Pneumoencephalography in the diagnosis of cerebral atrophy. Utrecht, the Netherlands: Drukkerij, Smits Oudergracht, 1959
- Bruni JE (1998) Ependymal development, proliferation, and functions: a review. *Microsc Res Tech* 41:2-13

Bruni JE, Del Bigio MR, Clattenburg RE (1985) Ependyma: normal and pathological. A review of the literature. *Brain Res* 356:1-19

Bull J (1956) The normal variations in the position of the optic recess of the third ventricle. *Acta Radiol* 46:72-80

Burhenne HJ, Davis W. The ventricular span in cerebral pneumography. *AJR* 1963; 90: 1176-1184

Cala LA, Thickbroom GW, Black JL, Collins DWK, Mastaglia FL. Brain density and cerebrospinal fluid space size: CT of normal volunteers. *AJNR* 1982;2:41 - 47

Connolly E, McKhann GI, Choudhri T, Huang J (2002) Fundamentals of operative techniques in neurosurgery. Thieme, New York

Corrales M, Torrealba G (1976) The third ventricle. Normal anatomy and changes in some pathological conditions. *Neuroradiology* 11:271-277

Dandy WE (1918) Ventriculography following the injection of air into the cerebral ventricles. *Ann Surg* 68:5-11

Engeset A, Lonnum A. Third ventricles of 12 mm width or more. *Acta Radiol (Stockh)* 1958;50: 5-11

Erdogan AR, Dane S, Aydin MD, Ozdikici M, Diyarbakirli S (2004) Sex and handedness differences in size of cerebral ventricles of normal subjects. *Int J Neurosci* 114:67-73

external ventricular drain placement. *Neurosurgery* 63:ONS162-166; discussion ONS166-167

Flyger G, Hjelmquist U (1957) Normal variations in the caliber of the human cerebral aqueduct. *Anat Rec* 127:151-162

Frazier C, Gardner W (1928) The radical operation for the relief of trigeminal neuralgia. *Surg Gynecol Obstet* 47:73-77

Gabrion JB, Herbute S, Bouille C, Maurel D, Kuchler-Bopp S, Laabich A, Delaunoy JP (1998) Ependymal and choroidal cells in culture: characterization and functional differentiation. *Microsc Res*

Gawler J, duBoulay GH, Bull JHD, Marshall J. Computerized tomography: a comparison with pneumoencephalography and ventriculography. *J Neurol Neurosurg Psychiatry* 1976;39:203- 211

Germany 44. Todd RB (1847) The cyclopaedia of anatomy and physiology. Longman, London

Graham J, Babalola KO, Honer WG, Lang D, Kopala L, Vandorpe R (2006) Lateral asymmetry in the shape of brain ventricles in control and schizophrenia groups. *Biomedical Imaging: Nano to Macro, 2006 3rd IEEE International Symposium, Arlington, VA*, p414

Greenberg MS (2010) Handbook of neurosurgery. Thieme, New York

Gyldensted C. Measurements of the normal ventricular system and hemispheric sulci of 100 adults with computed tomography. *Neuroradiology* 1977;14: 183-192

Hahn FJY, Rim K. Frontal ventricular dimensions or. Normal computed tomography. *AJR* 1976;126:492-496

Haug G. Age and sex dependence of the size of normal ventricles on computed tomography. *Neuroradiology* 1977;14:201-204

his life, discoveries, and contributions to our understanding of the nervous system. *J Neurosurg* 114:268-272

Horbar JD, Leahy KA, Lucey JF (1983) Ultrasound identification of lateral ventricular asymmetry in the human neonate. *J Clin Ultrasound: JCU* 11:67-69

Ito M, Hatazawa J, Yamaura H, Matsuzawa T. Age-related brain atrophy and mental deterioration—a study with computed tomography. *Br J Radio/1981* ;54:284-390

Jean WC, Abdel Aziz KM, Keller JT, van Loveren HR (2003) Subtonsillar approach to the foramen of Luschka: an anatomic and clinical study. *Neurosurgery* 52:860-866, discussion 866

Kakarla UK, Kim LJ, Chang SW, Theodore N, Spetzler RF (2008) Safety and accuracy of bedside

Kaufmann GE, Clark K (1970) Emergency frontal twist drill ventriculostomy. Technical note. *J Neurosurg* 33:226-227

Kawashima M, Li X, Rhoton AL Jr, Ulm AJ, Oka H, Fujii K (2006) Surgical approaches to the atrium of the lateral ventricle: microsurgical anatomy. *Surg Neurol* 65:436-445

Keen WW (1890) Surgery of the lateral ventricles of the brain. *Med News* 57:275-278

Key A, Retzius MG (1875) Studien in der Anatomie des Nervensystems und des Bindegewebes,

Kido DK, LeMay M, Levinson AW, Benson W. Computed tomographic localization of the precentral gyrus. *Radiology* 1980;135 :373-377

Kiroglu Y, Karabulut N, Oncel C, Yagci B, Sabir N, Ozdemir B (2008) Cerebral lateral ventricular asymmetry on CT: how much asymmetry is representing pathology? *Surg Radiol Anat: SRA* 30:249-255

Kremen WS, Panizzon MS, Neale MC, Fennema-Notestine C, Prom-Wormley E, Eyler LT, Stevens A, Franz CE, Lyons MJ, Grant MD, Jak AJ, Jernigan TL, Xian H, Fischl B, Thermenos HW, Seidman LJ, Tsuang MT, Dale AM (2012) Heritability of brain ventricle volume: converging evidence from inconsistent results. *Neurobiol Aging* 33:1-8

Krokhors G, Katila O, Taalas J (1967) Enlarged suprapineal recess of the third ventricle. *Acta Neurol Scand* 43:607-615

Le Gars D, Lejeune JP, Peltier J (2009) Surgical anatomy and surgical approaches to the lateral ventricles. *Adv Tech Stand Neurosurg* 34:147-187

Lee CK, Tay LL, Ng WH, Ng I, Ang BT (2008) Optimization of ventricular catheter placement via posterior approaches: a virtual reality simulation study. *Surg Neurol* 70:274-277, discussion 277-

Leite Dos Santos AR, Fratzoglou M, Perneczky A (2004) A historical mistake: the aqueduct of Sylvius. *Neurosurg Rev* 27:224-225

LeMay M, Hochberg FH. Ventricular differences between hydrostatic hydrocephalus and hydrocephalus ex vacuo by computed tomography. *Neuroradiology* 1979;17: 191-195

LeMay MJ. Neurological aspects of language disorders in the elderly. An anatomical overview. In: Obler LK, Alber ML, eds. Language and communication in the elderly. Lexington, MA: Heath, 1980: 107-119

Longatti P, Fiorindi A, Feletti A, D'Avella D, Martinuzzi A (2008) Endoscopic anatomy of the fourth ventricle. J Neurosurg 109:530-535

Longatti P, Fiorindi A, Perin A, Martinuzzi A (2007) Endoscopic anatomy of the cerebral aqueduct. Neurosurgery 61:1-5, discussion5-6

Lowery LA (2008) Mechanisms of brain ventricle development. Massachusetts Institute of Technology, Cambridge

Magendie F (1828) Mémoire physiologique sur le cerveau40. Rogers L (1931) The foramen of Magendie. J Anat 65:457-467

Matsushima T, Rhoton AL Jr, Lenkey C (1982) Microsurgery of the fourth ventricle: Part 1. Microsurgical anatomy. Neurosurgery 11:631-667

McRae DL, Branch CL, Milner B (1968) The occipital horns and cerebral dominance. Neurology 18:95-98

Meese W, Kluge W, Grumme TT, Hopfermuller W. CT evaluation of the CSF spaces of healthy persons. Neuroradiology 1980;19 :131-135

Menovsky T, De Vries J, Wurzer JA, Grotenhuis JA (2006)

Mestres P (1998) Introduction to histology of the ventricular wall of the brain. Microsc Res Tech 41:1

Monro AS (1783) Observations on the structure and functions of the nervous system. Creech & Johnson, Edinburg

Morton LT (1954) Garrison and Morton's Medical Bibliography. Grafton, London

Paine JT, Batjer HH, Samson D (1988) Intraoperative ventricular puncture. Neurosurgery 22:1107-1109

Park YG, Woo HJ, Kim E, Park J (2011) Accuracy and safety of bedside external ventricular drain placement at two different cranial sites: Kocher's point versus forehead. J Kor Neurosurg Soc 50:317-

Pellicci LJ, Bedrick AD, Cruse RP, Vannucci RC. Frontal ventricular dimensions of the brain in infants and children. Arch Neurol 1979;35 :852-853

Placement of ventricular drains—Kocher, Frazier, and Paine's points. http://www.brain-surgery.us/Drain_Placement.html

Reichert KB (1861) Der Bau des menschlichen Gehirns. Engelmann, Leipzig

Rhoton AL Jr (2002) The lateral and third ventricles. Neurosurgery 51:S207-271

Ross MH, Pawlina W (2006) Histology: a text and atlas: with correlated cell and molecular biology. Lippincott Williams & Wilkins, Philadelphia

Sabattini L. Evaluation and measurements of the normal ventricular system and subarachnoid spaces by CT. Neuroradiology 1982; 23:1-5

Sadler TW (2006) Langman's medical embryology. Lippincott Williams & Wilkins, Philadelphia

Schiller F (1997) the cerebral ventricles. From soul to sink. Arch Neurol 54:1158-1162

Sharifi M, Ungier E, Cizek B, Krajewski P (2009) Microsurgical anatomy of the foramen of Luschka in the cerebellopontine angle, and its vascular supply. *Surg Radiol Anat: SRA* 31:431-437

Sharp JA (1961) Alexander Monro Secundus and the interventricular foramen. *Med Hist* 5:83-89

Snell RS (2010) *Clinical neuroanatomy*. Wolters Kluwer Lippincott Williams & Wilkins, Philadelphia

Spiller WG (1916) Syringomyelia. Syringoencephalomyelia. *J Nerv Ment Dis* 44:395-414

Standring S (2008) *Gray's anatomy: the anatomical basis of clinical practice*. Churchill Livingstone, Edinburgh

Stefini R, Rasulo FA (2008) Intracranial pressure monitoring. *Eur J Anaesthesiol Suppl* 42:192-195

Steno A, Popp AJ, Wolfsberger S, Belan V, Steno J (2009) Persisting embryonal infundibular recess. *J Neurosurg* 110:359-362

Strauss E, Fitz C (1980) Occipital horn asymmetry in children. *Ann Neurol* 8:437-439

Synek V, Tuben JR, duBoulay GH. Comparing Evan's index and computerized axial tomography in assessing relationship of ventricular size to brain size. *Neurology (NY)* 1976 ;26:231-233

Taboada D, Alonso A, Alvarez JA, Paramo C, Vila J (1979) Congenital atresia of the foramen of Monro. *Neuroradiology* 17:161-164
Tech 41:124-157

Tillmanns H (1908) Something about puncture of the brain. *Br Med J* 2:983-984

Timurkaynak E, Rhoton AL Jr, Barry M (1986) Microsurgical anatomy and operative approaches to the lateral ventricles. *Neurosurgery* 19:685-723

Tubbs RS, Loukas M, Shoja MM, Shokouhi G, Oakes WJ (2008) Francois Magendie (1783-1855) and his contributions to the foundations of neuroscience and neurosurgery. *J Neurosurg* 108:1038-1042

Tubbs RS, Vahedi P, Loukas M, Shoja MM, Cohen-Gadol AA (2011) Hubert von Luschka (1820-1875):

Turkewitsch N (1935) Die Entwicklung des Aquaeductus cerebri des Menschen. *Morphol Jahrb* 76:421-447

Turkewitsch N (1936) Die Entwicklung des subkommissuralen Organs beim Bind (Bos taurus L.). *Morphol Jahrb* 77:573-586

ventricles in autism. *Psychiatry Res* 163:106-115

Vidal CN, Nicolson R, Boire JY, Barra V, DeVito TJ, Hayashi KM, Geaga JA, Drost DJ, Williamson PC, Rajakumar N, Toga AW, Thompson PM (2008) Three-dimensional mapping of the lateral

Virchow R (1854) *Handbuch der speziellen Pathologie und Therapie*, Berlin

von Gerlach J (1858) *Mikroskopische Studien aus dem Gebiete der menschlichen Morphologie*. Enke, Erlangen

von Luschka H (1855) *Die Adergeflechte des menschlichen Gehirnes: eine Monographie* Reimer, Berlin

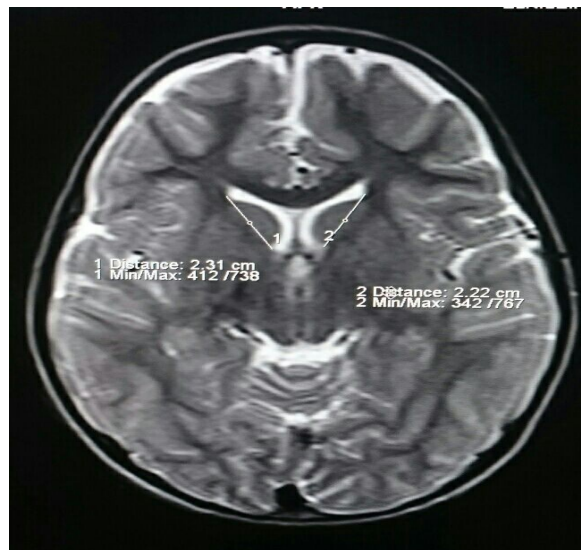
Wolpert SM. The ventricular size on computed tomography. J Comput Assist Tomogr 1977;2:222-226

Wollam DH, Millen JW (1953) Anatomical considerations in the pathology of stenosis of the cerebral aqueduct. Brain 76:104-112

Zatz LM, Jernigan TL, Ahumada AJ Jr. Changes on computed cranial tomography with aging. Intracranial fluid volume. AJNR 1982;3 : 1- 11

Appendices

Image.1 measurement of rt and lf frontal horns at level of



interventricular foramen

image.2 . Measurement of lateral ventricles width and length at



most widening area

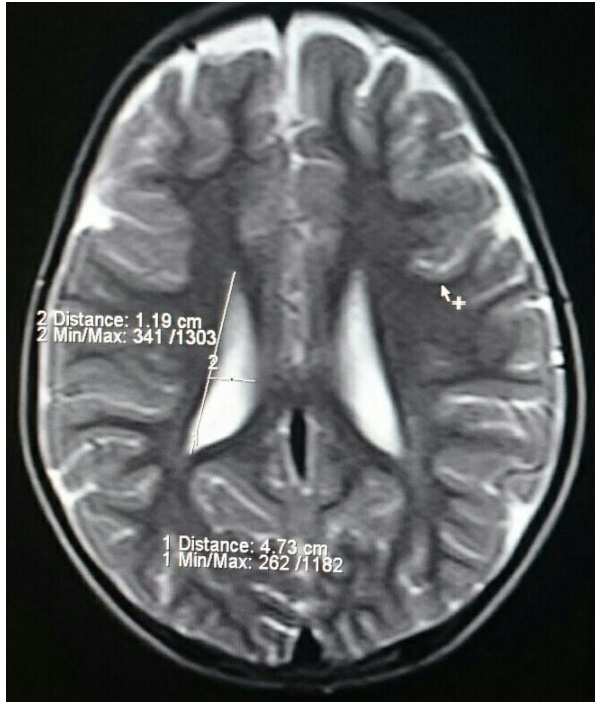


Image.3. Measurement of forth ventricle



Image.4. Measurement of aqua duct



Image.5. Measurement of BPD

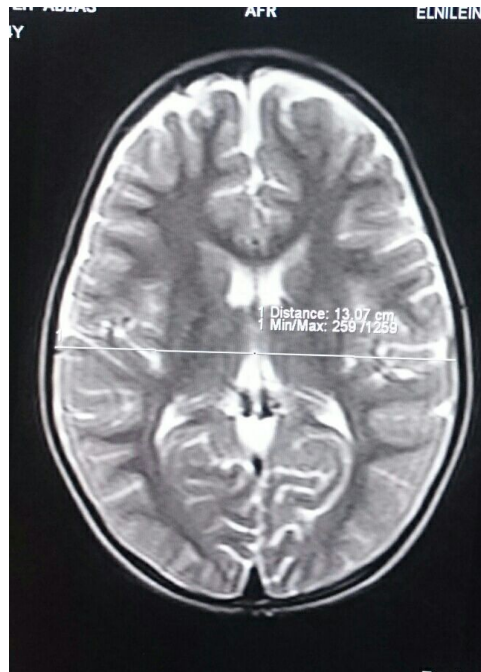


Image.6. Measurement of rt and lf anterior to posterior horn

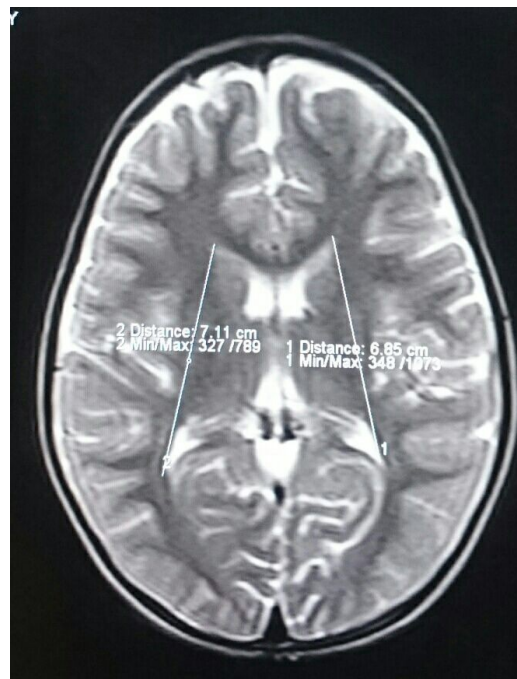


Image.7. Measurement of third ventricle at level of interventricular foramen



